UNIVERSITÀ DEGLI STUDI DI PADOVA

DIPARTIMENTO DI INGEGNERIA DELL'INFORMAZIONE

University of Basel
Department of Biomedical Engineering

DIPARTIMENTO DI INGEGNERIA DELL'INFORMAZIONE

CORSO DI LAUREA IN BIOINGEGNERIA INDUSTRIALE

"Implementation and testing of an improved haptic feedback for a Robotic Endoscopy System Based on Series Elastic Actuation "

"Implementazione e testing di feedback aptico per sistema di endoscopia robotica basato su Series Elastic Actuation (SEA) "

Relatore: Prof. Giulio Rosati

Laureando/a: Sara Lisa Margherita Ettori

Correlatore: Ing. Matteo Bottin
Prof. Georg Rauter
Ph.D. Lorin Fasel
Dr. sc. Nicolas Gerig

ANNO ACCADEMICO 2023 –2024

Data di laurea 11.04.2024

Abstract

0.1 English abstract

The lab where I am doing my thesis has previously developed a novel endoscopic system for safer neurosurgery. The main goal was to reduce interaction forces between the instrument and brain tissue thanks to springs in the transmission between the motors and the movable endoscope tip. Furthermore, the interaction forces can be estimated by measuring the deflection of the springs. To make the telemanipulation of that robotic system safer and more intuitive for the surgeon, they implemented force feedback: When colliding with brain tissue while telemanipulating the robot, the surgeon can now ”feel” this interaction through a haptic input device. However, the force feedback implementation was only a proof-of-concept prototype and should be improved for a future clinical application. Therefore, my project was focused on the implementation and evaluation of an improved haptic feedback system. The thesis was divided into three main work packages. Firstly, the haptic input device was tested by evaluating delays, both in the communication between the different systems and in the motor control, and the quality of the force rendering. Secondly, I explored options for the mapping between endoscope tip force measurements and force commands to the haptic input device. These algorithms aim to recreate the sensation of touch and force for the surgeon during surgery. Lastly, a user study was carried out to evaluate the final product. Non-medical researchers with an engineering background were recruited for this pilot study to evaluate the usability of the implemented system and whether it fits the imposed requirements. The implemented haptic feedback shows statistically significant results both in reducing time and torques, all by remaining under the force limits imposed by literature. Furthermore, users show higher confidence when using haptic feedback and have a lower error rate. In conclusion, the promising results are a solid starting point for future work and for a more relevant system evaluation.

0.2 Italian abstract

Il laboratorio dove sto facendo la tesi ha precedentemente sviluppato un nuovo sistema endoscopico per una neurochirurgia piu' sicura. L'obiettivo principale era quello di ridurre le forze di interazione tra lo strumento e il tessuto cerebrale grazie alle molle nella trasmissione tra i motori e la punta dell'endoscopio mobile. Inoltre, le forze di interazione possono essere stimate misurando la deformazione delle molle. Per rendere la telemanipolazione del sistema robotico piu' sicura e intuitiva per il chirurgo, hanno implementato il feedback di forza: quando si scontra con il tessuto cerebrale mentre telemanipola il robot, il chirurgo puo' ora "sentire" questa interazione attraverso un dispositivo di input tattile. Tuttavia, l'attuale implementazione del feedback di forza e' solo un prototipo di proof-of-concept e dovrebbe essere migliorato per una futura applicazione clinica. Pertanto, il mio progetto si concentra sull'implementazione e la valutazione di un sistema di feedback tattile migliorato. La tesi e' suddivisa in tre pacchetti di lavoro principali. In primo luogo, il dispositivo di input tattile viene testato valutando i ritardi, sia nella comunicazione tra i diversi sistemi che nel controllo del motore, e la qualita' del rendering della forza. In secondo luogo, vengono esplorate le opzioni per la mappatura tra le misure della forza di punta dell'endoscopio e i comandi di forza al dispositivo di input aptico. Questi algoritmi mirano a ricreare la sensazione di tocco e forza per il chirurgo durante l'intervento chirurgico. Infine, viene effettuato uno studio per valutare il prodotto finale. Ricercatori non medici con un background ingegneristico sono reclutati per questo studio pilota per valutare l'usabilita' del sistema implementato e se soddisfa i requisiti imposti. Il feedback aptico implementato mostra risultati statisticamente significativi sia nella riduzione dei tempi che dei momenti, il tutto rimanendo sotto i limiti di forza imposti dalla letteratura. Inoltre, gli utenti mostrano una maggiore sicurezza quando utilizzano il feedback aptico e hanno un tasso di errore inferiore. In conclusione, i risultati promettenti rappresentano un solido punto di partenza per il lavoro futuro e una valutazione del sistema piu' rilevante.

Acknowledgements

I am thankful to Professor Georg Rauter for providing me with the opportunity to be a part of the lab and for offering invaluable inputs throughout the project. Special thanks are due to Professor Giulio Rosati from the University of Padova whose support made this experience possible.
I would like to express my deepest gratitude to my supervisors, Lorin Fasel and Nicolas Gerig, for their support, guidance, and insights throughout the last six months. Their dedication and expertise have been instrumental in shaping the direction of this thesis.

I extend my appreciation to all the PhD candidates of the BIROMED-Lab for always offering help and support when needed.
Furthermore, I would like to acknowledge my fellow master students Nico, Nico and Costi for their every day encouragement, and friendship.

University of Basel
Department of Biomedical Engineering

BIROMED-Lab
Medical Robotics and Mechatronics

Master Thesis: Haptic Feedback for a Robotic Endoscopy System Based on Series Elastic Actuation

Context:
In the BIROMED-Lab, we take inspiration from nature to develop robots that assist surgeons during their interventions. In one project we have been developing an endoscopic system for safer neurosurgeries with inspiration from human finger anatomy. Thanks to springs in the transmission between the motors and the movable endoscope tip, the interaction forces between the instrument and the brain tissue can be reduced. Furthermore, the interaction forces can be estimated by measuring the deflection of the springs. To make the telemanipulation of that robotic system safer and more intuitive for the surgeon, we implemented a force feedback: When colliding with brain tissue while telemanipulating the robot, the surgeon can now "feel" this interaction. However, the current force feedback implementation is only a proof-of-concept prototype and should be improved for a future clinical application.
Task description: Your task will be to implement an improved haptic feedback and evaluate it with regards to performance metrics such as usability, force fidelity, and safety.

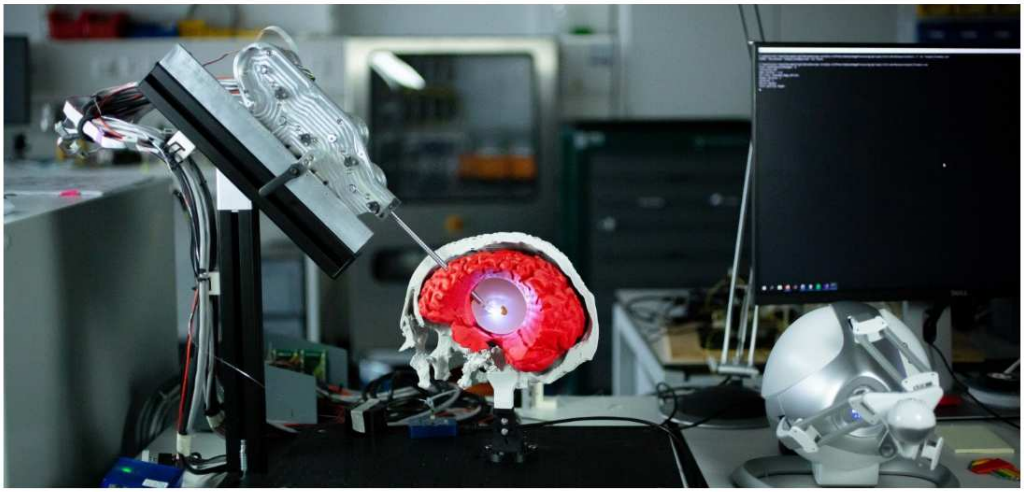

Workpackages:

- Literature research and concept development: Get familiar with the existing system and the topic of haptic feedback.
- Implementation: Develop a control algorithm that renders haptic feedback to the surgeon using a suitable haptic input device.
- System evaluation: Come up with a test strategy to evaluate the technical aspects of the system.
- (Optional) User study: Evaluate the usability of your approach in a small study.

Student: Sara Ettori
Start: Sept. 2023
Duration: 6 months

https://biromed.dbe.unibas.ch

Supervision:
Lorin Fasel
Nicolas Gerig
Professor: Prof. Dr. Georg Rauter

Contents

List of Figures

List of Tables

1 Introduction

Brain surgery, also known as neurosurgery, is a medical specialty that involves the treatment of conditions affecting the brain, spinal cord, and peripheral nerves. Each year, over 13 million patients worldwide require some neurosurgical care. The current deficit in neurosurgical care is around 5 million cases a year [7]. Over the years, significant advancements in technology and surgical techniques have transformed the landscape of brain surgery, enabling more precise interventions and improved patient outcomes. However, this field also faces numerous challenges, ranging from ethical considerations to technical complexities. In recent years, a shift has occurred in neurosurgical techniques, marked by a transition towards minimally invasive procedures (Fig. 1.1, left). Manual endoscopic surgery has redefined the field, minimizing tissue trauma and scarring while expediting patient recovery [8, 9]. Inherent risks persist in neurosurgery despite strides in minimally invasive techniques. Complications such as infections, bleeding, and damage to surrounding structures necessitate constant vigilance and precise management. Accessibility remains a challenge in ensuring neurosurgical care. Abandoning open brain surgery has, on the other hand, brought to light different drawbacks: first of all, the maneuverability/dexterity at the surgical location has decreased. Furthermore, the surgeon's physiological hand tremors are enhanced since the surgeon holds the endoscope for long hours and usually in difficult-to-maintain positions. Lastly, using the endoscope has completely eliminated the possibility for the surgeon to feel the tissue he is working on with the endoscope. Haptic feedback (the ability to feel the forces being applied) is of utmost importance in brain surgery because of the extremely delicate tissues the surgeon is dealing with and the enormous damage that could result from a lesion or even a rupture of said tissues. Therefore, introducing robots in neurosurgery has been considered (Fig. 1.1, right). This technological synergy holds the promise of improved surgical outcomes and reduced risks. Furthermore, since the surgeon does not operate the endoscope directly but via telemanipulation, the robot can filter out the surgeon's hand tremors [10]. Even if the general aim for robotic surgery would be to lower the costs and improve the patient's outcome by maintaining the whole procedure safe [11], robots still need to be completely trusted by surgeons and patients. One aspect that mines the safety of the procedure is the absence, to this day, of haptic feedback; in this thesis, I improved and evaluated the haptic feedback capabilities of a previously developed robotic system for minimally invasive neurosurgeries.

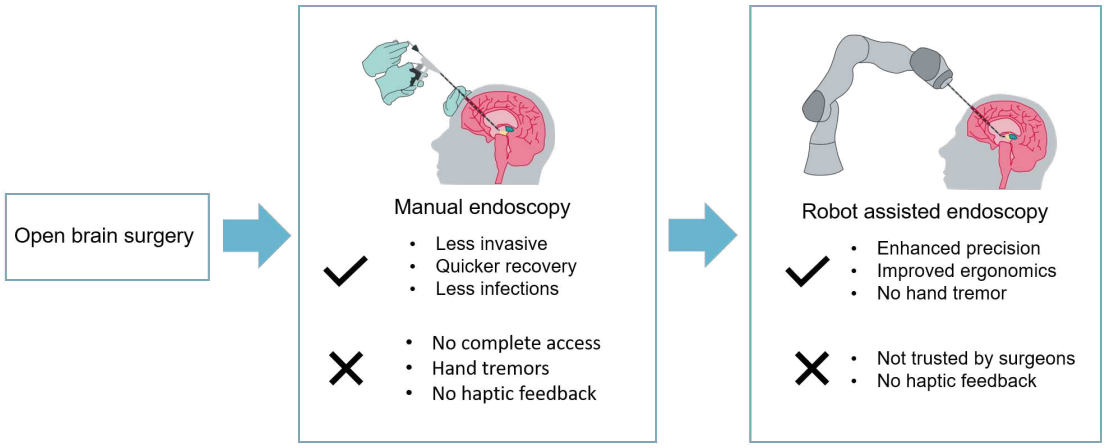

Figure 1.1: Advantages and disadvantages of laparoscopic surgery, and robot-assisted surgery in the scenario of brain surgery [1]

1.1 Minimally invasive surgery

Minimally invasive surgery (MIS) refers to surgical techniques that minimize or even eliminate incisions on the patient's body. Laparoscopic MIS has been favored over conventional open surgery in the past decades due to the reduction in trauma and blood loss, permitting the patient to recover quicker and with fewer complications and infections [8]. Nevertheless, laparoscopic surgery poses notable challenges for surgeons. These encompass a constrained field of vision and operational space stemming from smaller incisions, the absence of tactile feedback, diminished hand-eye coordination attributed to specialized equipment, a steep learning curve necessitating prolonged training periods, and extended procedure durations owing to intricate surgical protocols. Over the past two decades, substantial attention has been directed towards developing robotic surgical systems to aid surgeons in minimally invasive procedures and enhance surgical ergonomics within confined workspaces.[12]

1.2 Medical robotics

In recent decades, integrating robotics into various fields has ushered in transformative changes and brought great advances in technology and research. Even if the advancement started later in medicine and has inevitably grown much slower than in other fields, it still holds a high potential. It is pushing the knowledge about robotics to its boundaries. To make an example, the Da Vinci robot (Intuitive Surgical, Sunnyvale, CA, USA) [13], the most spread out robot in the world for robot-assisted surgery, restores the degrees of freedom (DOFs) lost with traditional laparoscopy, permitting to have movement of the end effector extremely similar to the one of a human wrist [14]. Adopting robotic systems in surgery

represents a leap forward, which could improve patient outcomes. Several key factors underscore the significance of robotics in surgery:

- Precision and Accuracy: The robotic systems are equipped with advanced sensors and imaging technologies, providing surgeons with a three-dimensional, high-definition view of the surgical field. This enhanced visibility, coupled with robotic arms that can move with a high degree of skill, allows for meticulous and precise maneuvers within the human body [15].

- Minimally Invasive Procedures: Surgeons can deploy robotic instruments with remarkable precision through smaller incisions, reducing trauma to surrounding tissues. Patients benefit from faster recovery times, diminished postoperative pain, and a lower risk of complications, all contributing to an overall improved quality of care [16]. More than laparoscopic procedures, robotic surgery assures better access to the different tissues that must be accessed and, simultaneously, assures a higher risk assessment and dealing. Robot-assisted microinvasive surgery (RAMIS) has yet to be applied to every sphere of surgery, and it is usually only used for orthopedics and torso surgery.

- Training and Skill Development: Surgical robotics facilitates structured training programs for surgeons. With simulation capabilities, aspiring and practicing surgeons can refine their skills in a risk-free environment. This not only accelerates the learning curve but also ensures a higher level of competence when transitioning to real-world surgeries.[17]

- Optimized Patient Outcomes: Ultimately, the integration of robotics in surgery is geared towards optimizing patient outcomes. From oncological procedures to cardiovascular surgeries, robotic assistance allows for greater surgical precision, reduced complications, and faster recovery times. These factors collectively contribute to improved patient safety and satisfaction.

The field of robotics applied to medicine, and more specifically to surgery, has been growing steadily for the last 20 years, bringing enormous changes to how we view all sides of medicine, from diagnostics to rehabilitation. The growth has been slower than in other fields, such as industrial production, where robotics were inserted at a certain time. Compared to most other fields, introducing robots in a medical environment requires more testing. It has to fulfill delicate safety requirements regarding materials, hardware, and software. All these aspects make it more difficult to combine medicine and robotics. Furthermore, the resistance of medical staff has also been a key factor in slowing down the growth and development of these technologies. Since the first robot was introduced in an operating room more than 30 years ago [18], technologies have developed and become much more sophisticated and

extremely appealing for all that they bring to the field, refer to [19] and [20] for a complete review on surgical robotics.

1.3 What is haptic feedback?

In human-robot interaction, the integration of haptic feedback has emerged as a revolutionary factor, bringing a sense of touch to machines. Haptic feedback refers to the technology that allows users to feel and manipulate virtual or remote objects through the sense of touch. This immersive sensory experience is transforming various fields, and one particularly promising application lies within the domain of surgical robotics.
Haptics can be divided in two main branches [21, 22]:

- Cutaneous: regards tactile sensations such as texture, shape, temperature, and vibrations. Specific sensors and organs in the skin sense these. Cutaneous cues do not affect the stability of the closed loop system, but they still can improve the system's transparency [23, 24, 25].

- Kinestethic: regards forces, torques, and body positions in space. These quantities are sensed by proprioceptors in the human body's muscles, joints, and tendons. The purpose of force feedback is to evaluate forces and tendons that are being applied by the user on the object being investigated. Increased force feedback gains make the teleoperation more transparent (precise force detection and no time delays), but the higher the transparency, the higher the consequent instability of the closed loop[26].

In general robotics, haptic feedback is pivotal in enhancing user control and precision. Whether in virtual reality simulations, gaming controllers, or teleoperation systems, the integration of haptic technology provides a more immersive and realistic experience by conveying the feel of surfaces, textures, and forces. In surgical robotics, applying haptic feedback takes on a profound significance. While offering higher precision, traditional robotic surgery often lacks the direct tactile feedback that surgeons rely on during traditional procedures. Haptic feedback in surgical robotics aims to recreate the tactile sensations experienced during manual surgery, closing the loop between the surgeon and the robotic instruments. The absence of the information usually received through the sense of touch also causes experienced surgeons to tear tissues because of the excessive force being applied at the surgical site [27]. Surgical robots with advanced haptic systems would help surgeons by allowing them to feel tissues' resistance, texture, and contours in real-time. Surgeons could rely on a more comprehensive set of sensory information, transcending the limitations of visual and

auditory cues alone. This enhances their skill and facilitates a smoother transition from traditional open surgeries to minimally invasive techniques. As stated in [28]. The introduction of haptic feedback, particularly in robot-assisted minimally invasive surgery, has proven to lower the peak forces that are being applied during the task, increase success rates, and reduce the time to complete the task.

Incorporating haptic feedback in surgical robotics benefits the surgeons, both during the surgery and during the training. However, it is proven that the learning curve with haptic feedback is quicker [29].

Haptic feedback becomes even more important when dealing with teleoperations, operations where the surgeon controls remotely, with the use of a haptic input device (leader robot), the surgical device (follower robot); in this case, any information that the surgeon receives are only based on visual or auditory cues and their knowledge [22].

2 Background and Motivation

Even if haptic feedback in robotics, and especially in robot-assisted surgery, has the potential to improve surgeons' outcomes, performance, and learning curves, its integration in the operating room is complex. The complexity comes from challenges that will be described in the following chapter and the technical complexity of achieving high transparency with a stable closed loop.

2.1 Requirements for haptic feedback in surgical robotics

The aspects of haptic feedback that must be considered when implementing a system are various and of various entities and complexity; the whole system, though, aims, in general, to be as transparent and stable as possible. It is also important to determine the most pressing problems to solve for the specific scenario in which the haptic feedback is used. For haptic feedback in brain surgery, the following aspects were addressed and researched:

- Delay: A very important aspect to consider is the delay in acceptable communication when working with haptic feedback. As reported in [22], [30] and [31], delays of 50ms can already be harmfully by altering the perception of stiffness: tissues are perceived softer when time delays increase [32]. The delays could be caused by different factors, such as communication or even the time needed by the haptic input device to achieve the desired forces [33]. Furthermore, delays could also cause instability in the loop [34]. All these aspects will be evaluated in the following chapter.

- Range of force feedback: During surgeries, particularly brain surgeries, very low forces are being applied, in the range of just a couple of newtons [35]. It should be noted that even though most tissues involved in the surgery are soft, high-stiffness tissue may exist in the workspace, such as bone structures or other surgical tools. Therefore, the system should also remain stable under hard-contact conditions[22] As stated in [36], most mistakes during surgery happen because of an excessive force being applied by the surgeon on the interested tissue. For the haptic feedback to be as reliable as possible, the specific surgical task's requirements must be considered to determine the desired force feedback capability and resolution for the haptic interface.

Thus, the haptic device's characterization is necessary and will be addressed in Chap. 4.

- Stability: Dynamic interaction forces can challenge the stability of a closed loop that controls the interactions between the haptic input device, the robot, and the remote environment. When dealing with surgical teleoperations, the challenge of stability intensifies as it concerns three separate systems: the human operator, the robot, and the environment. These systems interact, exchanging energy[36]. Because of the bidirectionality of this exchange, further attention has to be put on the stability of the whole system. The system's stability is linked to its transparency, and a trade-off between these two features has to be found to make the feedback as helpful as possible [16].

- Friction: when working with both a leader and follower robot, the joint frictions of both have to be taken into account since they inevitably alter the force sensing and rendering. In the endoscope, which will be described in the following, the friction occurs at several stages of the joint, including the actuator that moves the tendon, the joint of the manipulator driven by the tendon, and the pulleys that support the tendon [37]. A friction compensator could be introduced to eliminate the effects of friction. Still, its modeling is challenging since it requires a deep understanding of the exact dynamics of the system. The friction of the leader robot will be evaluated during the test in Chap. 4.

- Magnification: In MIS, the interaction forces involved are often well below the human perception. For this reason, amplifying the interaction force can allow the user to perceive and safely apply delicate forces traditionally interpreted only from visual feedback. A scaling factor or gain has to be determined based on the specific requirements of the procedure and the haptic input device used for the surgery [36, 38]. The chosen gain can not be too high since it would severely mine the system's stability, especially when dealing with hard contact.

2.2 State of the art of haptic feedback in robotic-assisted surgery

In general, the whole system can be divided into three different sections:

- Follower robot: in this scenario, the endoscope used for palpation in brain surgery,
- Leader robot: the haptic input device controlled by the user,
- Communication: which protocol ensures fast and effective communication between the two.

The following section will briefly summarize these three parts and their state of the art; for a more detailed overview, refer to [22, 21, 39] for the state of the art of haptic feedback in robotic surgery and to [40] for haptic interfaces and user's performance.

Figure 2.1: Da Vinci set up an operating room. (a) Follower robot, (b) leader robot.

Follower robot or patient side robot

Concerning the patient-side robot, (a) in Fig.2.1, a further challenge must be overcome: measuring the contact forces between the instrument and the tissue.
Classical force torque sensors are usually too big and would make the surgical tool impractical. Furthermore, tools used during surgery must be biocompatible and sterilized before each use. Thus, this process should be as easy as possible and should not involve the waste of precious or expensive materials.
There are two different approaches to measuring the contact force:

- Direct force sensing [41, 42, 23]: with the use of sensors of different physical nature, contact forces can be measured directly and sent to the haptic device. For a detailed

explanation of all the different types of sensors, with their advantages and drawbacks, refer to [2]. Furthermore, the position of said sensor is of the utmost importance since it changes the nature of the force that is being sensed, the different possible positionings of sensors on the Da Vinci shaft are shown in Fig. 2.2.

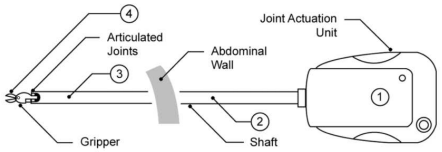

Figure 2.2: Different possible positions for force sensors [2]

- Force estimation: using a deep learning algorithm from imaging [43] or estimating instrument force using external force sensors [44, 45, 46], this approach is also the one used in the endoscope based on series elastic actuation that will be the starting point for this thesis work [47, 48], this system will be explained in more detail in the following.

The two previously mentioned approaches could be addressed by sensorizing existing robotic systems. Many different attempts of adding sensors, for example, to the Da Vinci robot, could be found in literature [49, 41, 23], see Fig.2.3 for an example; or by developing a new endoscope that allows the measurement, directly or indirectly, of contact forces at the surgical site [47, 50, 44]

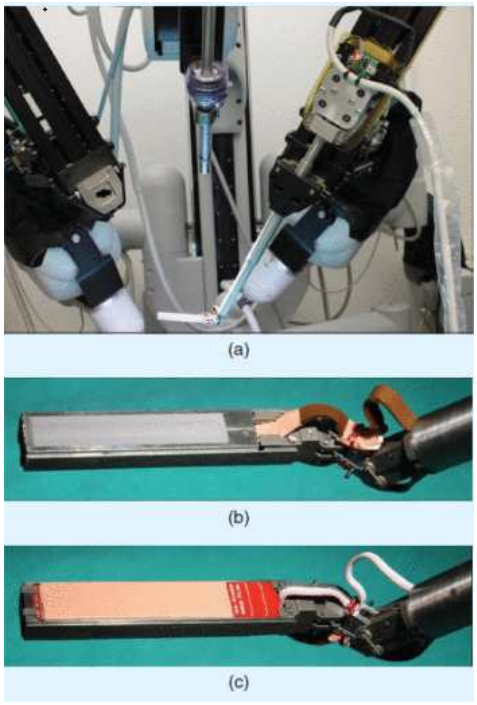

Figure 2.3: Example of sensorization of Da Vinci end effector[3] using piezoresistive (b) and capacitive (c) sensing methods

Leader robot or surgeon side robot

When talking about haptic feedback, not only is it fundamental to have a device that can detect the forces at the site of contact between tissue and tool, such as the ones previously described, but it is also necessary to have a haptic input device that covers the role of leader robot (b) in Fig.2.1. The user can telemanipulate the endoscope and receive feedback on the forces the follower robot measures. It is possible to find many of these haptic input devices on the market, each with different characteristics [51, 52]. Most commercially available ones are meant for gaming purposes, making them only sometimes adequate for surgical applications but having really low prices. As stated in [22], the haptic interface must comply with many requirements. Depending on the specific scenario, the task that must be done, and the tissues involved, different aspects must be considered more important than others. For example, when dealing with the palpation of the brain tissue, the force range doesn't necessarily have to be very wide since the forces are really low and the damaging forces are extremely similar to the average forces; values are reported in Tab. 2.1. For this scenario, it is more important that the rendering of the measured forces allows the user to detect the difference between tissues with similar stiffness. Information about the evaluation of the rendering capabilities of the available devices is scarce and not always consistent [53, 54]. Therefore, in the following chapters, I set up my experiments to evaluate the Novint Falcon (Novint Technologies, Albuquerque, New Mexico, USA). Different authors have also devel-

oped their own haptic devices tailored to the application of robotic surgery [55, 56]. This would be out of the scope of the thesis; I decided to use affordable and easy-to-implement solutions to see what was possible to do with it.

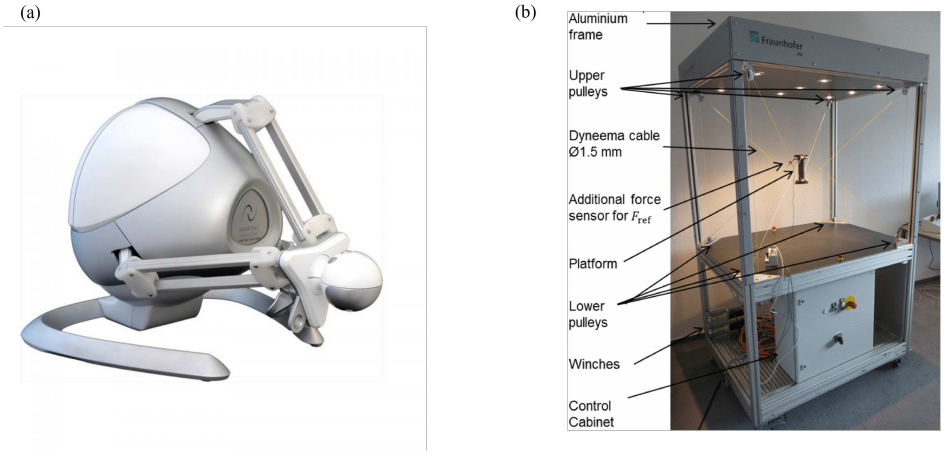

Figure 2.4: Haptic input devices. (a) Nonvit Falcon, (b) newly developed cable-driven haptic input device (right) [4]

Communication

The third and last component of the closed loop in haptic feedback is the communication protocol used to ensure the transfer of information between the two robots. Generally, the leader will give information about the position to the follower, who will send back information regarding the forces at the surgery site. As previously stated, this information exchange must be as fast as possible for stability reasons and to ensure that the user receives information that helps improve the procedure's outcome. For real-time communication, such as the one necessary for haptic feedback, a commonly used protocol is UDP, which ensures a communication delay of a couple of milliseconds [57, 58]. The following chapters will investigate this aspect as a preliminary test.

2.3 Background for the thesis and its objectives

Figure 2.5: (a) Overview of the whole system, (b) disassembled motor attached to each tendon, (c) zoom on endoscope's tip. [5]

The overall project will be briefly described in the following section, explaining the reasoning for the new endoscope, how it works, and its novelties. The paragraph summarizes the following papers [47, 48, 59, 5]. Refer to said papers for the exact calculations and a more in-depth system description.
As previously discussed, the main feature lacking in robotic surgery is haptic feedback. The endoscope will shortly be described, and this thesis aims to try and fill the said gap by estimating the forces from the spring deflection and subsequently making them perceivable to the user controlling the endoscope through the haptic device.

For RAMIS (robot-assisted minimally invasive surgery) to be as precise and reliable as possible, the endoscope has to be maneuverable, and the tip must move with at least one degree of freedom. Since the endoscope tip has to be as small as possible, its movement is usually controlled by external motors, which then transfer the movement to the tip through tendons. By integrating a rotational spring with a known torque-deflection curve between the end-effector and the motor, it is possible to measure the spring deflection and estimate the torques being applied at the tip of the endoscope. This type of actuation is known as Series Elastic Actuation (SEA), and it increases safety during the robot's interaction with the environment [60], by lowering the contact forces. The stiffness of the spring is a function of the deflection since it's nonlinear. It is defined as the derivative of the torque-deflection curve concerning the deflection [5] to comply with the impact forces measured during brain surgery and reported in Tab. 2.1.

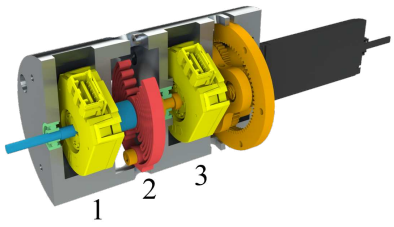

Figure 2.6: Zoom on the detail of the actuation on each tendon of the endoscope. (1) Load side encoder, (2) non-linear spring, (3) motor side encoder. [5]

Since one aim of the novel neuroendoscope is to achieve a variable stiffness at the tip, non-linear springs (2 in Fig.2.6) with the following torque-deflection curve are used:

$$\tau_q = c_s \cdot (\Delta q)^2 \tag{2.1}$$

Where τ_q is the spring's torque, c_s is the constant of the spring, and Δq is the deflection of the spring. From the torque of the spring, it is possible to calculate the tendon force as follows

$$F_{t,ij} = \frac{\tau_{q,ij}}{r_w} \quad where \quad \tau_{q,ij} = c_{s,ij}(q_{m,ij} - q_{l,ij})^2 \tag{2.2}$$

Where r_w is the winch radius, $q_{m,ij}$ is the position of the encoder on the motor side (3 in Fig.2.6), and $q_{l,ij}$ is the position of the encoder on the load side (1 in Fig.2.6). Combining the two indexes $i, j = 1,2$ represents the four different tendons. By pulling on the tendons, the joints on the endoscope will move and generate a torque. The tendon force will then close the inner loop of Fig. 2.7. The estimated angle of the joint can be calculated with the forward kinematics, given the position of the encoder on the load side.

$$\hat{\phi} = Jq_l \tag{2.3}$$

Where J is the Jacobian matrix. The estimated position is then confronted with the desired one, the joint torque is calculated, and the torque of the actuator is determined. Said torque is then mapped to a desired force on the tendon $F_{des,ij}$, closing the outer loop of Fig. 2.7.

Having information about the force applied on the tendon F_t; it is easy to determine the estimated torque at the joint $\hat{\tau_\phi}$; the only thing needed is information about the lever arm, which depends on the contact point between endoscope and tissue. The value was estimated at $l_c = 0.01m$.

Maximum Forces [N]	Average Forces [N]	Damaging Forces [N]
2	0.86	1.14

Table 2.1: Applied forces during brain surgery [6]

The advantages of this new actuation are various:

- mechanical compliance, lower forces applied during surgery, and quicker response to impact,
- precise measurement of joint position,
- force sensing at the surgical site.

Having information about the forces being applied at the tip of the endoscope makes it interesting to see if they can be used to give force feedback information to the user. To do so, the torques calculated are given as input to a haptic device and said torque would be mapped to forces on the device to make the feedback reliable and useful. To close the haptic loop (the third loop in the control scheme in Fig. 2.7), the position of the haptic device is determined and sent back and used as an input for the control as the desired position.

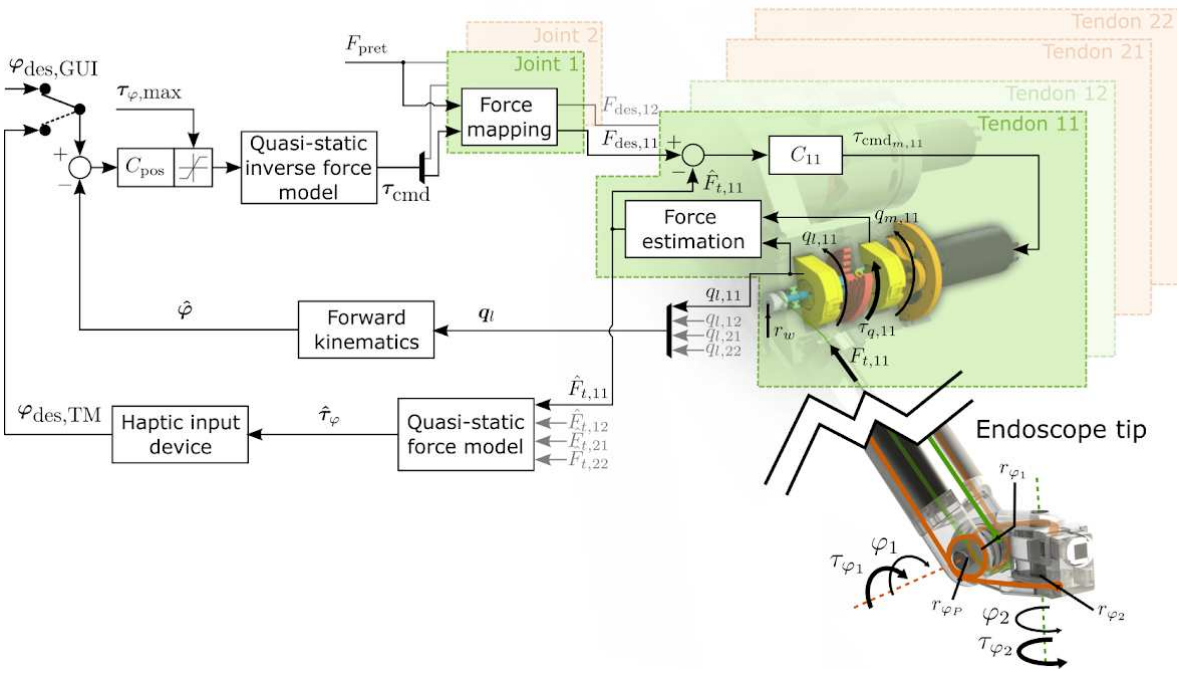

Figure 2.7: Control scheme of the SEA-based endoscope image by Lorin Fasel [5]

The following thesis work will focus on the implementation and testing of this last feature and will be structured as follows:

- preliminary tests of the haptic device and communication,
- mapping techniques based on previous tests,
- small user study to evaluate the overall product,
- limitations and future work.

3 Materials and Methods: Hardware evaluation

As a starting point of the thesis work, the communication protocol had to be changed from ADS to UDP and tested; secondly, the leader robot had to be characterized to ensure it complied with the specific requirements.

3.1 Data transmission

3.1.1 System implementration

To test the delays in communication, the following setup was used:

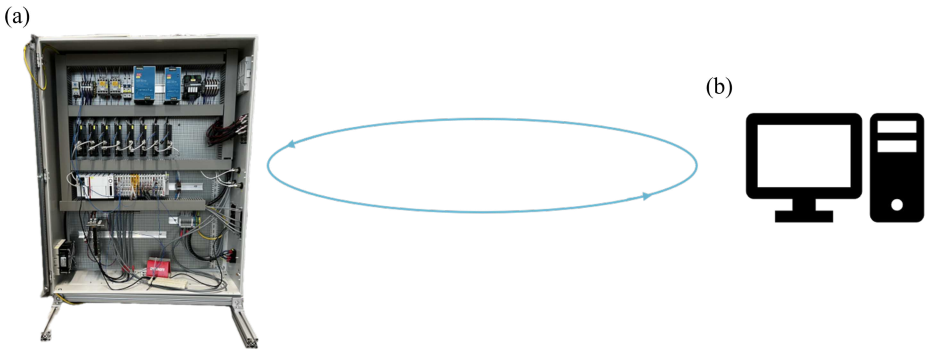

Figure 3.1: System for the Communication test. (a) Real-time PC, (b) computer.

The system control was running on two different machines: a real-time PC based on TwinCAT3 (Beckhoff Automation, Verl, Germany), running a PLC and a C++ program (also controlling the endoscope), and a workstation PC, running a C++ program. A UDP connection, which replaced the pre-existing ADS one, was established between them to ensure the correct communication between the two computers, and that data was sent back and forth between them. UDP, which stands for User Datagram Protocol, is one of the core protocols of the Internet Protocol (IP). It is a connectionless transport protocol, meaning that it does

not establish a connection before sending data and does not guarantee the delivery or order of the data, making it extremely fast. Because of its speed and simplicity, UDP is commonly used in real-time applications where low latency is crucial, making it interesting for our application in haptic feedback. Delays and latency have to be as low as possible to have a force rendering that is as realistic as possible and be sure not only to add to the surgeon's experience but also not to be harmful or misleading.

3.1.2 Test procedure

Using one of the C++ Force Dimension SDK examples, it was possible to read the coordinates of the handle of the Falcon every millisecond (refresh frequency of the Falcon) and store it in a variable of type structure containing the three separate values (p_x, p_y, p_z). Said structure is then sent, with a specific code line, to the target, the RT PC, via UDP in this scenario. The UDP socket was previously opened, and the IP addresses of both local and remote PCs and the receiving port (11000) were specified. On the receiving end (RT PC), a second C++ code running on Twin CAT mirrored the incoming data and sent it back to the Computer. The real-time PC refreshed every millisecond, meaning it could receive new data at that rate. This first test calculates the time the packet needs to complete a whole cycle, known as RTT (Round Trip Time). The packet is a structure of three doubles for a total of 24 bytes; this size was chosen accordingly to what will be needed in the next tests and the user study. To achieve the goal of accurately measuring the RTT, a clock was set to start every time data was sent from the computer to the RT PC and to stop when the Computer received the packet again. The process and the calculation were repeated several times to ensure the results were significant.

3.2 Haptic input device

3.2.1 System implementation

To test the hardware necessary for the tests, the following setup was built:

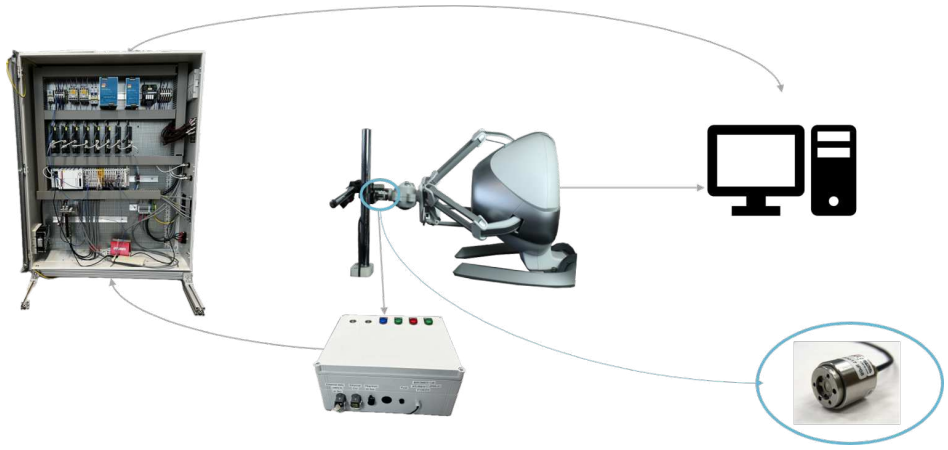

Figure 3.2: System set-up for Hardware test. (a) Real-time PC, (b) Nano 16 IP68 Force/-Torque sensor, (c) Falcon Haptic input device, (d) computer.

The haptic device chosen for the initial testing is the Novint Falcon, a 3D robotic haptic controller. Its three degrees of freedom, given by the three arms actuated by three different motors, allow the user to navigate easily the three-dimensional workspace. Said workspace is a cube of dimension 100mmx100mmx100mm. The Falcon's software keeps track of where the grip is moved and creates forces that a user can feel by sending currents to the motors in the device. The Falcon's sensors can keep track of the handle's position to sub-millimeter resolution, and the motors are updated 1000 times per second (1kHz). Nevertheless, the limits of this haptic device must be addressed and tested to verify its usefulness for our specific goal. Force Dimension (Nyon, Switzerland) offers an SDK (Software Development Kit) that allows one to easily control the chosen haptic device by only adding a few C++ lines to the provided code. Also, simple examples provided were used as a starting point for the applications.

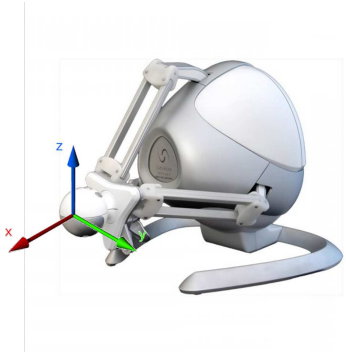

Figure 3.3: Falcon haptic device with axis.

The Falcon was connected to the computer via a USB cable, communicating via UDP with the real-time PC to receive data. Both the computer and the real-time PC are the same as in the previous section.

A force/torque sensor was attached to the handle to determine the forces along the three principal axes rendered by the Falcon. The sensor was the Nano 17 IP68 (ATI Industrial Automation, Apex, NC, U.S.A.). Given the specifications, this type of sensor was more than accurate enough for our purposes. The calibration SI-50-0.5 (maximum forces on x and y of respectively 50N and 70N for z and a resolution of 1/80 in all three directions), provided by the constructor, was chosen. Only the forces were needed for the tests, and we were not interested in the torques since the Falcon, whose rendering we were evaluating, could not generate them.

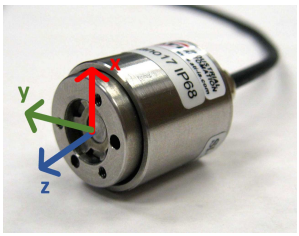

Figure 3.4: Nano 17 IP 68 force and torque sensor with axis

The sensor is connected to the real-time PC via an Ethernet cable to close the communication loop. The tool side (shown in Fig. 3.4 with the references to the axis) was attached to the Falcon's handle, while the cable side was attached to the control box. The latter was connected to the real-time PC via an Ethernet cable to close the communication loop.
An adaptor was needed to attach the sensor to the Falcon's handle, see Fig. 3.5. Since no adaptor specific to this scenario was available on the market, a new one had to be designed using Solid Works and 3D printed in ABS (Acrylonitrile butadiene styrene). Other scenario-specific pieces were also designed for correct testing. First of all, two blocks (Fig. 3.6) for

the base of the Falcon to block it to a thorLab Table (Thorlabs, Newton, New Jersey, USA) of size 300mm x 450mm (Fig.3.8 (b)), secondly a block for the sensor (Fig.3.7)to attach it to three degrees of freedom adjustable articulated support (Fig.3.8 (a)), attached on the other side to the table. To attach objects to the table, M6 screws were used, and to attach objects to the sensor, M3 screws were used.

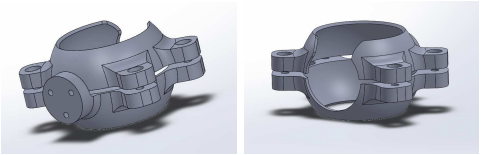

Figure 3.5: Solidworks CAD of adapter to attach the sensor to the handle of the Falcon

Figure 3.6: Solidworks CAD of the block to fix the falcon to the table

Figure 3.7: Solidworks CAD of adapter to attach the sensor to the articulated arm.

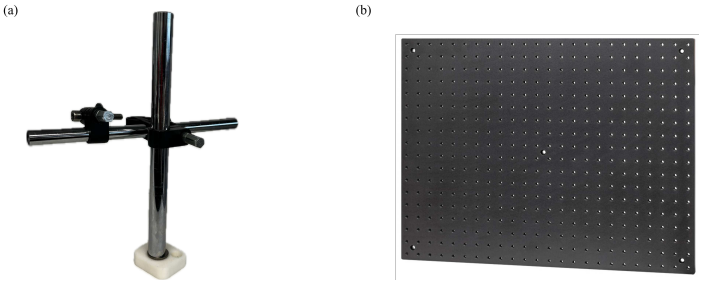

Figure 3.8: (a) Three degrees of freedom adjustable articulated arm and (b) thorLab table.

3.2.2 Test procedure

Secondly, the choice of using the Falcon as a haptic device had to be tested to see if it was in line with our specific goals; in particular, what we are looking to find out with the test is how good the rendering of the Falcon is and the delay in said rendering.
The idea behind the necessity of testing the Falcon is that, first of all, in the literature, many

aspects of the Falcon's force rendering weren't present, especially when using a Force and Torque sensor and UDP connection; secondly, its results, we think, could give a strong basis for the following step: a correct mapping and choosing the right gain.
To do so, the Nano 17 IP 68 force sensor was mounted, with the use of the adaptors previously described on the handle of the falcon; on the other side, the sensor was blocked to the ThorLAB table with the use of the degrees of freedom adjustable articulated support, making it easy to adjust and change the position of the falcon. For the falcon to stay still when applying the different forces, its base was also blocked on the table. Given the described setup, it was then possible to start the testing process. The first step was to set up the communication between the different parts; the sensor was connected through an Ethernet cable to the RT PC, and the Falcon was connected via USB to the local computer. As previously mentioned, the communication between the two computers was via RT UDP. Two separate codes were running on the two computers to control the sensor and the Falcon separately. On the remote computer, a PLC code was implemented to, on one side, read the data from the force sensor and plot it on a YT Scope project and, on the other hand, generate a function to be sent to the local computer at a frequency of 1kHz via UDP, and simultaneously plot it on the same YT Scope Project as the forces detected by the sensor. On the computer, a C++ code was implemented to receive the function from the remote computer, interpret it as a force, and apply said force to the falcon through specific codes provided again by the Force Dimension SDK. To ensure that the Falcon can render forces adequately to our goals, two things were tested and evaluated in particular:

- The delay given, not only by the communication but also by the falcon itself, is due to the time needed to actuate the motors and generate the forces being sent. Important to notice is that this delay, summed to the communication delay, must stay under a threshold of around 50ms for haptic feedback to be significant and useful.

- The rendering capability of the Falcon, lower and upper limits, and difference in magnitude between the commanded force and the one measured by the sensor.

Two different force profiles were commanded to the Falcon:

- Steps at different magnitudes to simulate hard contact at the endoscope tip, which, as previously discussed, is one of the major problems mining the stability of the whole system; therefore, an aspect that we have to investigate carefully and take into consideration while doing the mapping. The magnitude varied between 1N and 21N, with an increment step of 1N.

- Sine waves (at different frequencies and amplitudes) to analyze the frequency response of the Falcon and, simultaneously, detect the minimal forces that the Falcon can render.

These aspects will be fundamental when deciding the correct force mapping. The amplitude was varied between 1N and 21N with an increasing step of 1N; the frequency was varied between 2 rad/s and 17 rad/s, with an increasing step of 0.5 rad/s.

These tests were carried out in different workspace positions, see Fig. 3.9 and Fig.3.10, since the rendering changes depending on whether the handle is in the center of the workspace or at its limits. Also, the rendering along the three axes is different. Even though the y- and z-axis behavior is of greater interest for our two-degrees-of-motion endoscope, the rendering along the x-axis was evaluated for completeness.

Figure 3.9: Side view of the Falcon when at the limit of the workspace for the x-axis

Figure 3.10: Front view of the Falcon when at the limit of the workspace for y-axis and z-axis

As shown in Fig.3.4 and 3.3, the Falcon and the force sensor have different reference systems, so to be sure that the two reference systems match, it was necessary to rotate one of the sensors to make it overlap the Falcon's one. To do so, we have to do a simple rotation of the coordinates, knowing that:

$$\begin{bmatrix} x_{sensornew} \\ y_{sensornew} \\ z_{sensornew} \end{bmatrix} = \begin{bmatrix} x_{falcon} \\ y_{falcon} \\ z_{falcon} \end{bmatrix} \tag{3.1}$$

Then:

$$\begin{bmatrix} x_{falcon} \\ y_{falcon} \\ z_{falcon} \end{bmatrix} = \begin{bmatrix} 0 & 0 & -1 \\ 0 & 1 & 0 \\ 1 & 0 & 0 \end{bmatrix} \begin{bmatrix} x_{sensor} \\ y_{sensor} \\ z_{sensor} \end{bmatrix} \tag{3.2}$$

The generated force was then set on one axis at a time to study and evaluate the rendering for each specific direction separately. Even though the endoscope is a two-degree-of-freedom device, the data we receive from the real-time computer regarding its position and torque is separated between the two.
Furthermore, in the user study carried out in the following, only one of the degrees of freedom (the first) will be evaluated, thus justifying the choice of studying the rendering on each axis separately.

4 Results and Conclusions: Hardware evaluation

4.1 Results and Discussion

4.1.1 Data transmission

The calculation of the RTT for each cycle was repeated many times to get a significant result, which permitted us to draw some preliminary but important conclusions. As previously mentioned, the delay of the whole haptic feedback has to be lower than 50 ms to make sure it's not harmful; for the total delay to be as low as possible, the first and easiest thing that can be changed is the communication protocol used, UDP is known to be extremely easy and fast making it perfect for real-time applications, such as this. The test results showed that even though the value of the RTT slightly varies, it remains below 3ms. It is important to note that the RT PC task runs at an update frequency of 1kHz, so we expect a delay of at least 2ms, one for the receiving and one for the sending. This first result is promising since we are over one order of magnitude under the problematic threshold of 50 ms, suggesting that this type of communication is working correctly and, secondly, is appropriate for haptic feedback in a brain surgery scenario.

4.1.2 Haptic input device

The following paragraph shows the results from the previously described test, which permits us to have a starting point for the second step of the project, which is the mapping and the user study.

Increasing step waves

Firstly, the approximate center of the workspace was tested. The exact center was impossible to achieve because of the physical and mechanical limits of the setup, especially the articu-

lated arm's mobility. The magnitude was increased by 2N every step; the frequency was set to 5Hz. The step wave with even and odd values was generated and sent to the falcon.

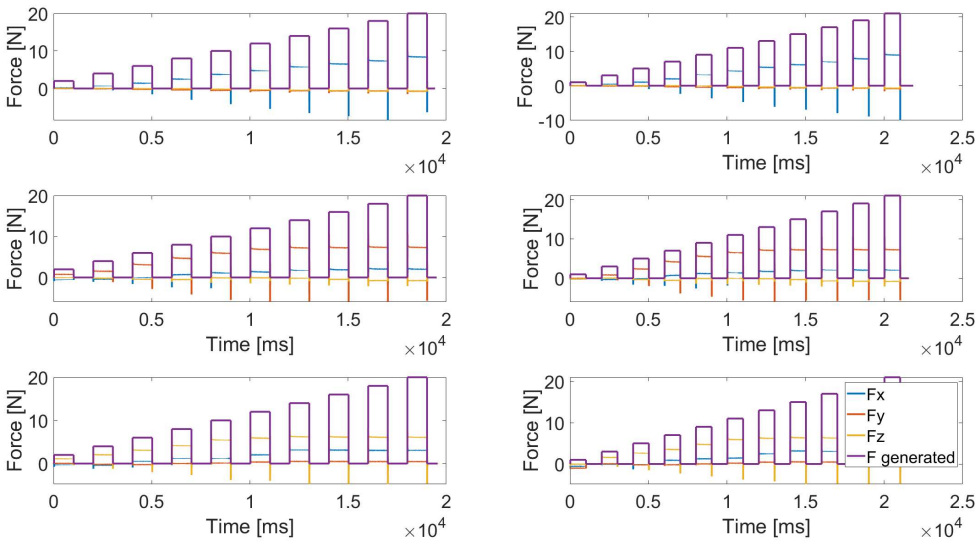

Figure 4.1: Generated and measured forces when imposing the force on the x-axis (top), on the y-axis (middle), and the z-axis (bottom). Steps of even value (left) and odd value (right). Central position of the Falcon in the workspace

Already from the plots in Fig.4.1, it is possible to make some remarks and interesting considerations:

The first thing that can be noticed is that the behavior along the three axes, x (top), y (middle), and z (bottom), is extremely similar. This consideration, along with the fact that for the mapping and the user study, we are initially only interested in the z- and y-axes, justifies the choice to analyze the behavior along one of said axes in the following paragraphs, the y-axis, in specific. Nevertheless, the tests were carried out for all three axes; the plots are in Appendix B.
The steps are divided between even and odd values only for computational reasons and to have neater plots.

Figure 4.2 shows a scatter-plot comparing the rendered force with the desired one.

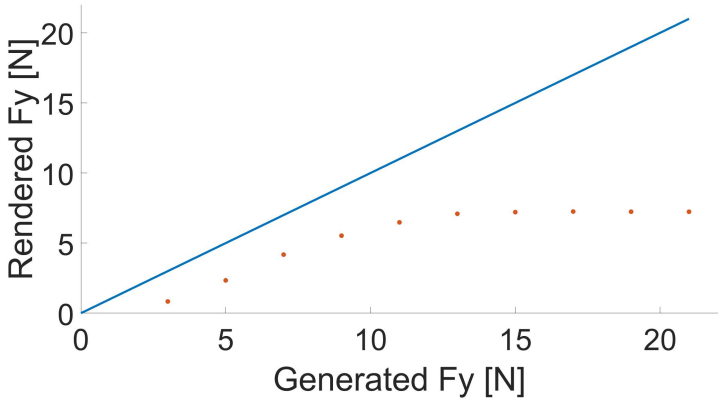

Figure 4.2: Scatter-plot of desired and rendered force on the y-axis. Theoretical line if there were no losses(orange), actual values (blue).

The shown scatter-plot was obtained by taking the middle point of each step to make sure the force was settled, since as shown in Fig. 4.1, there are positive and negative peaks when the force is imposed and taken away. The average time needed for the falcon to settle to the imposed force is of 61.8 ms.
From this scatter-plot and the previous one, two important pieces of information can be understood. First, there is an obvious rendering loss between the forces sent and imposed on the falcon and those measured by the force torque sensor. This loss is probably due to internal friction of the falcon motors that cannot render the desired force. Furthermore, at 14.9N of the desired force, the rendering stops following the desired one, settling at a much lower level at 7.2N. These values were obtained by interpolating the rendered force data points previously obtained, obtaining a continuous curve. To identify the value at which the rendering force saturates, the point where the difference between the y coordinate (rendered force) of said point and the following one was lower than 0.01N was selected. In the range where the force rendering is considered acceptable, between 1N and 14.9N for the desired force, the average percentage error was calculated, obtaining a value of 51.935% and a standard deviation of 15.4376%. The Average percentage error indicates that the rendering of the falcon cuts the desired force in half.
These results will have to be taken into account when doing the mapping, imposing an upper and lower limit on the forces that can be asked of the falcon to render. This will ensure that the haptic feedback during the tests does not require forces that are too high or too low to be rendered correctly.
Furthermore, the rendering changes when moving from the center to the limits of the workspace. As described in the previous chapter, the system's response to steps with increasing magnitudes was tested at different positions in the workspace.

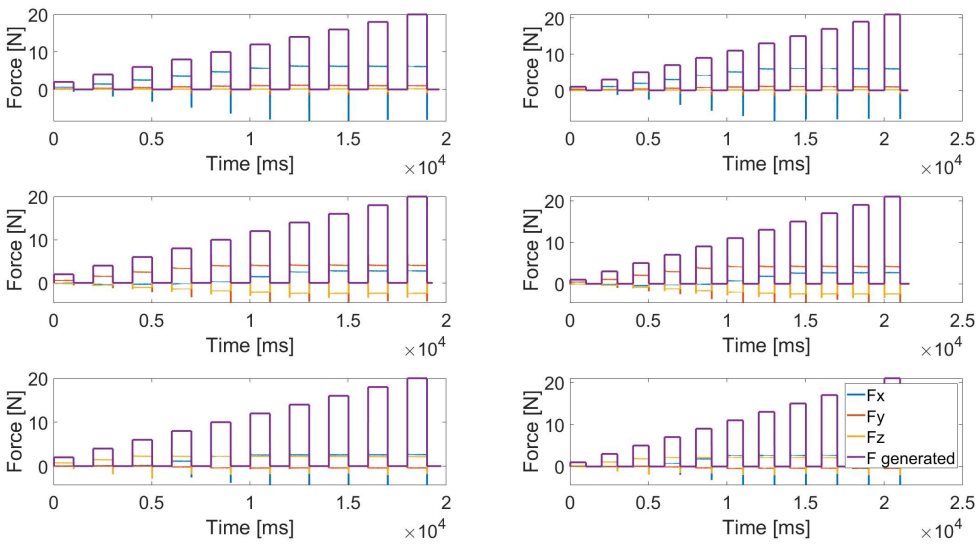

Figure 4.3: Desired and measured forces when imposing the force on the x-axis (top), on the y-axis (middle), and the z-axis (bottom). Steps of even value (left) and odd value (right). Falcon at the limit of the workspace for the y-axis and z-axis.

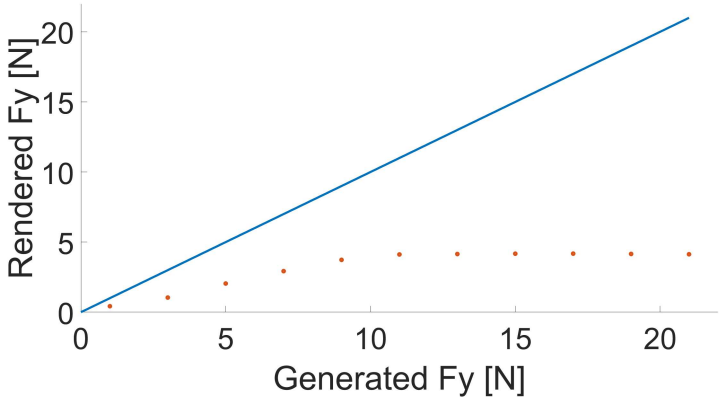

Figure 4.4: Scatter-plot of desired and rendered forces. Theoretical line if there were no losses(orange), actual values (blue).

As expected, the same conclusions as in the previous test can be drawn from the plots in Fig. 4.3 and 4.4. Still, with both the upper limit and the overall rendering loss due to friction being lowered by a couple of newtons, this lowering of the rendering capabilities at the edge of the workspace could be caused by the Jacobian having a different magnification effect on the sides of the workspace. Indeed, by following the same steps of interpolation previously described, we found a maximum desired force of 11.1N, which corresponded to a force of 4.1N in the rendered one. This shows a worsening in the rendering for two reasons: a lower overall achieved force and a higher multiplication factor to get the desired force

from the rendered one. This consideration is also supported by the mean percentage error of 60.4542% with a standard deviation of 2.2112%; the mean percentage error is much higher than in the central position. The same test was carried out for the limits of the x-axis while keeping the y-axis and z-axis as centered as possible; similar conclusions can be obtained.
These results justify the decision to do the following rendering tests only in the approximate center of the workspace since it is also the intended default position of the Falcon during the tests, thus being the position in which the rendering capabilities are more interesting. Also, this consideration will have to be taken into account when doing the position mapping for the haptic feedback; the mapping should prevent the Falcon from getting too close to the limits of the workspace since, in this position, the force rendering can not be considered reliable and could lead to mistakes of the user.
Next to the force rendering, the delay in the response of the falcon was investigated. This hardware-related delay adds to the communication delay (Section 4.1.1), bringing the total delay much closer to the previously mentioned threshold of 50ms. To do so, it was registered the instant in which the rendered force reaches the highest value (overshoot) and the one where the desired force goes from 0N to the set value, and the two were subtracted one from the other. The following graph shows the delay in milliseconds for each step:

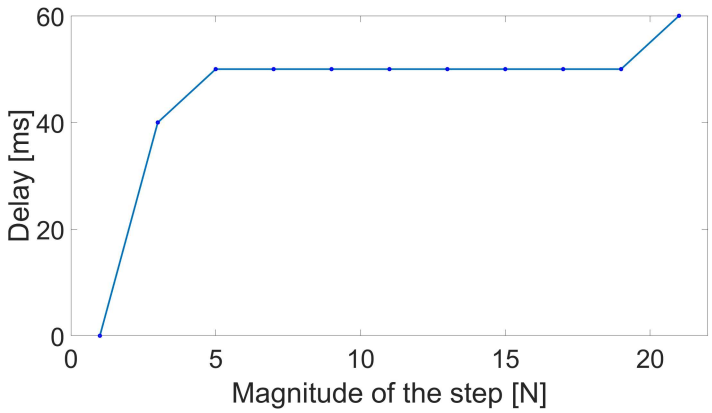

Figure 4.5: Calculated delay for each value of the steps.

The total delay grows by more than one order of magnitude when the falcon is asked to render forces due to the time required for its actuators (electric motors) to reach the desired torque. It has to be noted that the total delay reaches the threshold for the force range where the rendering is the most reliable. This has to be considered a limiting factor of the setup and must be considered when evaluating the user study. This problem could be solved by using a more refined haptic input device. Changing the device, though, was not in the scope of this master thesis.

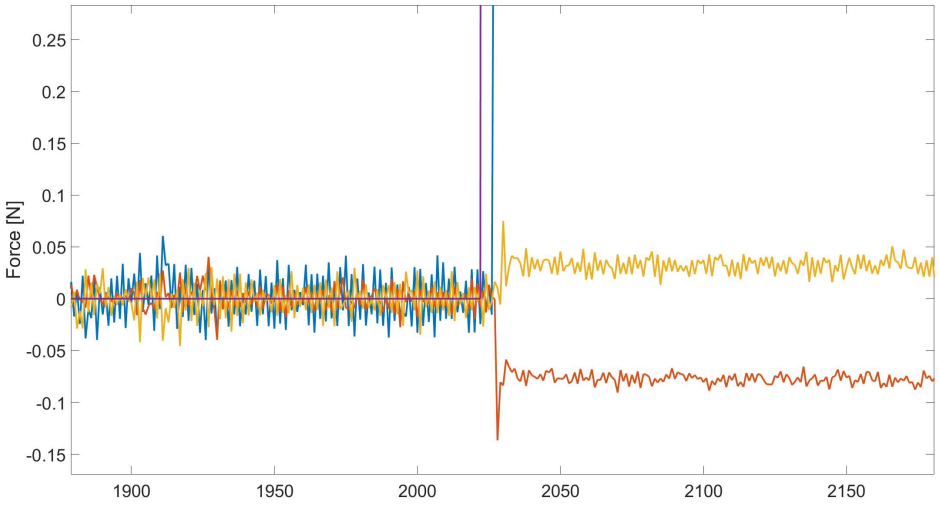

Figure 4.6: Zoom on the delay between the generated force signal (purple line) and outputs of the force sensor (blue, orange, and yellow line).

In Fig.4.6, a zoom on one of the steps of Fig.4.1 is reported to show clearly the delay there is between the generated step (purple line) and rendered and sensed forces (blue, orange, and yellow line).

Sine waves

As previously mentioned, different sine waves were also tested other than the steps. Again, the tests were carried out on all three axes, but only the results for the y-axis are shown in the following. The Falcon's handle was blocked in the central position for all the following tests.

At first, we generated a sine wave with a fixed frequency of 5Hz; the amplitude was increased by 0.5N every two periods, going from 0.5N to 14N, since the limit in the previous test for the rendering was indeed found when the generated force was at around 14N, making it useless to try and achieve higher forces.

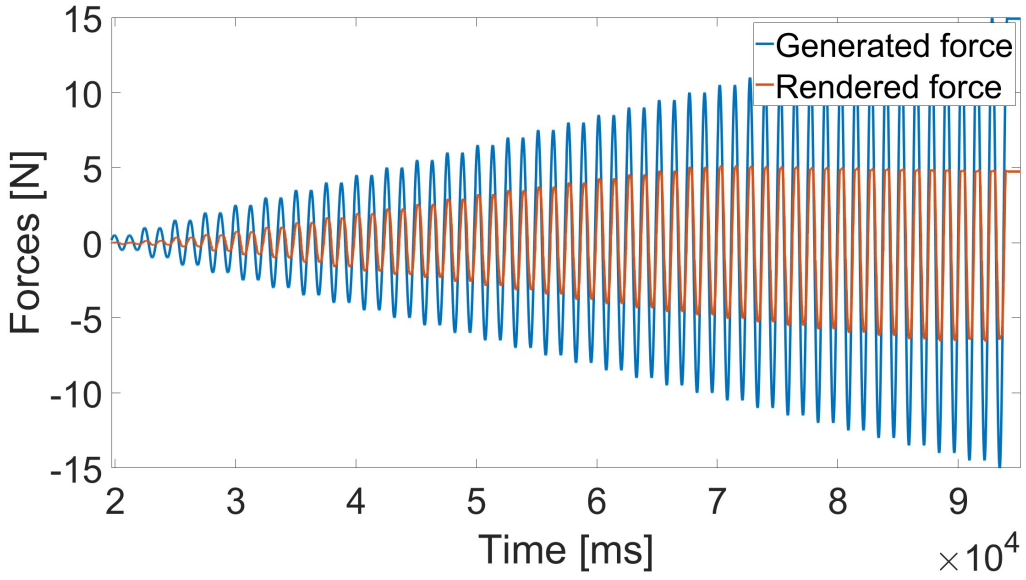

Figure 4.7: Desired and measured forces when generating a sine wave with increasing amplitude and fixed frequency and imposing it on the y-axis.

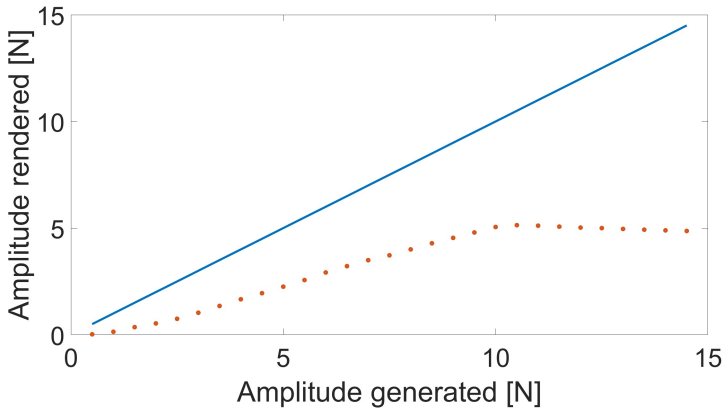

Figure 4.8: Scatter-plot of desired and rendered force.

From Fig. 4.7 and 4.8, it is possible to confirm the previous statement. It is possible to see how, even in the absence of hard contact and with varying forces, the limits of the rendering of the Falcon are the same as the one previously stated. With this test, it is possible to pinpoint the force at which the rendering saturates with a precision of 0.5N. Furthermore, from the scatter-plot obtained by taking the peak points of each couple of periods, it is also possible to draw similar conclusions as in the previous tests, with different limits. The rendering saturates at 5.1350N when the desired force reaches 10.5404N, lowering the upper limit from the previous test. Different factors could cause the higher loss in this case; when applying sine waves as commanded forces, the system changes speed and acceleration much quicker, causing an exacerbation of the effects of friction and thus lowering the rendering capabilities. The average percentage error in the interval [0.5, 10.5404] is 58.945% with a standard deviation of 12.054%.
The last thing left to investigate was the frequency response of the Falcon.

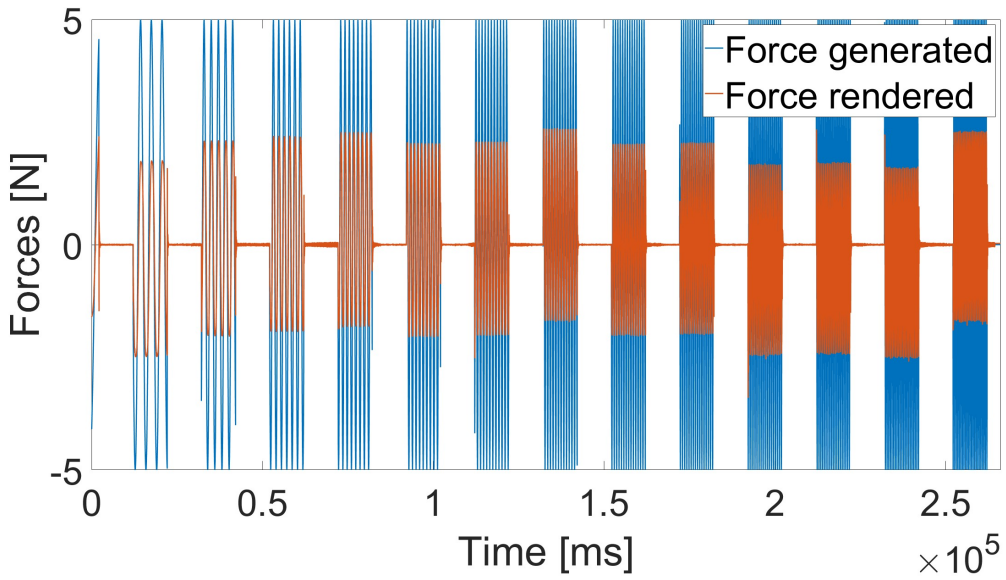

Figure 4.9: Desired and measured forces when generating a sine wave with increasing frequency and fixed amplitude and imposing it on the y-axis.

As predicted, the average measured amplitude of the sine wave is 2.3179N, which is exactly half of the desired one. This confirms once again the rendering loss caused by the Falcon. The average percentage error is 53.6419% with a standard deviation of 4.8599%. This test, though, was carried out to investigate the response of the Falcon when varying the frequency of the desired sine wave. For this purpose, the Bode plot was made :

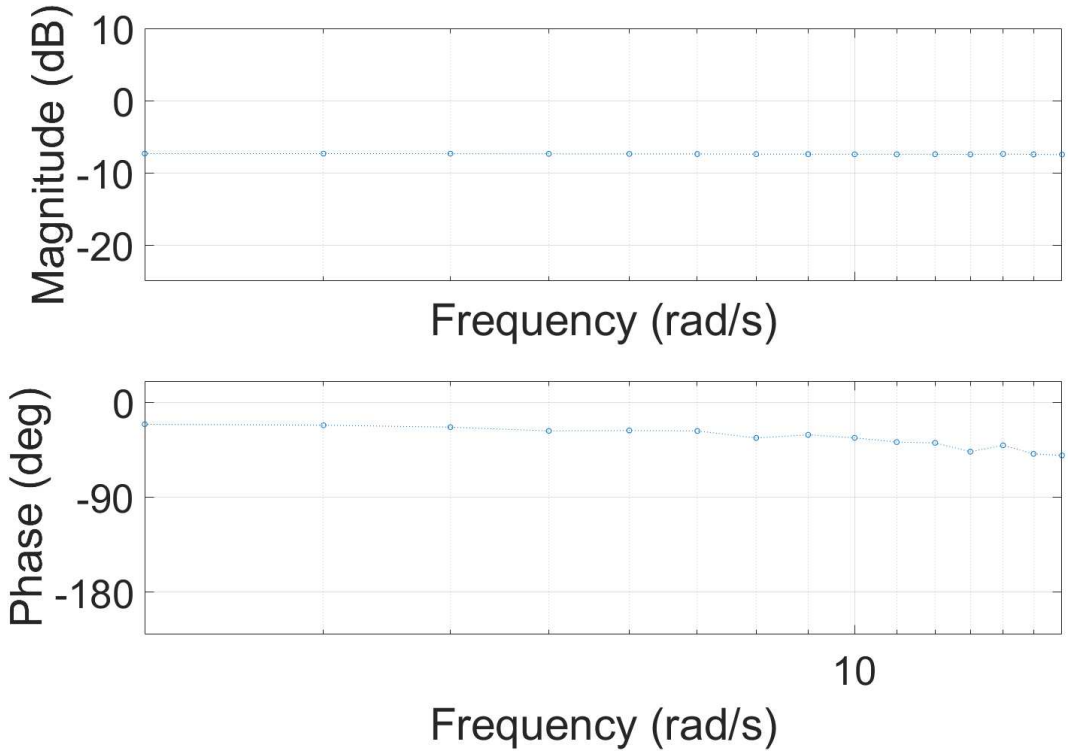

Figure 4.10: Bode plot for frequency response. Magnitude plot (top), phase plot (bottom).

The Bode diagram of the magnitude shows that the magnitude does not change with the frequency. Thus, we do not have to worry about varying losses for the frequencies we are testing, but we can correct the error with constant gain. In the Bode diagram, the phase (in degrees) represents the shift between the desired and rendered forces. A negative phase means the rendered signal is delayed in comparison to the generated one, which is taken as a time reference. From the graph, it's pretty obvious that there is a consistent delay in rendering the signal.

By looking at the time stamps of the peaks of the sine waves at different frequencies, what can be noticed is that the value of the delay, calculated as the difference between the time at which the desired wave reaches the peak and the time at which the rendered one reaches it, is pretty consistent independently from the frequency of the wave. Its values, as also for the step, vary between 30 ms and 60 ms, with an average of 50 ms, confirming the fact that also, in this scenario, the delay reaches the threshold and will have to be considered when evaluating the user study and the overall effectiveness of the haptic feedback. Looking at the Bode plot, it is possible to notice that the phase shift gets lower (higher absolute value). This happens because the delay in ms remains consistent, representing a bigger fraction of the sine wave. The phase shift must remain low because, in the proximity of the zeros, the force being rendered is in the opposite direction of the desired one. However, for the tested frequencies, the system remains stable. The frequency range that is being tested, even if it could appear

too slim to make a complete evaluation of the system, was caused by the test setup, which became unstable at higher frequencies because of the many parts being attached one the the other. The choice, though, was justified by the fact that human movement in general and even more in surgery, where movement is slower and more precise, is within these frequency limits [61].

4.2 Conclusion

The results previously shown will be summed up in the following paragraph, which will be the starting point for the second block of the work, which is the force and position mapping, which will be described in more detail in the following chapter.
The whole purpose of all the previous tests was to identify the limits both in time and rendering of the setup that will be used for the user study: the newly implemented UDP connection and the choice of using the Falcon as a haptic input device.

- Delay really close to the threshold of 50ms imposed by literature,
- For $F_{desired} > 14.9N$, rendering force saturates at $F_{sat} = 7.2N$, and for F desired $<$ 1.2N, rendering force is negative. This means that the mapping will have to stay between these two values to make sure all the forces that we are interested in feeling can be correctly identified and felt by the surgeon. When working with sine waves, the upper limit gets lower: $F_{desired} > 10.54N$ corresponding to $F_{sat} = 5.14N$
- Force losses get higher with higher forces; there is a linear dependency between the force being commanded and the desired one, meaning that the mapping will not necessarily need a nonlinear tendency. The choice will though depend also on other considerations that will be explained in the following chapter,
- In working frequencies, the phase does not decrease below -47.269°, meaning that in the human movement frequencies, there should not be any instability problems,
- Amplitude does not change in a significant way with different frequencies.

5 Material and Methods: User Study

5.1 Force and Position mapping

The following chapter will explain the user study we carried out. The chapter will be organized in the following way:

- Mapping techniques,
- Experimental setup,
- Study procedure.

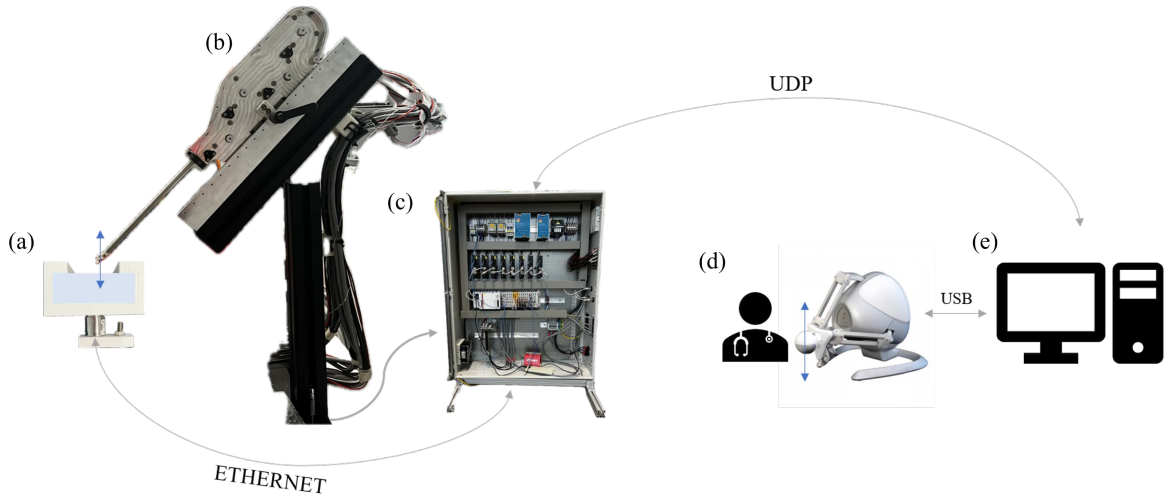

Figure 5.1: Overview of the whole setup for the user study. In gray, the physical cables connect the different parts. In blue, the movement of the falcon and the endoscope. (a) Sample and sample holder with the force sensor attached to the bottom, (b) SEA-based endoscope, (c) real-time computer, (d) Falcon haptic input device controlled by the user, (e) computer

To determine if the endoscope, the Falcon, and the chosen mapping are adequate for tissue palpation in brain surgery, a small user study was carried out. The aim was to verify if the

whole setup could detect contact forces at the tip and render them to the user in an easy, natural, and helpful way. To do so, the users, all non-surgeons with little to no training in handling haptic input devices, were asked to inspect a silicone sample in different scenarios and determine whether there was a plastic insertion under the contact point or not. The plastic insertion was meant to simulate tumors embedded in the brain tissue.

5.2 Force and Position mapping

The concept of mapping in haptic feedback involves establishing a correlation in both force and position between the leader robot, the Falcon manipulated by the user, and the follower robot, a 2-DOF endoscope based on SEA.
In our specific scenario the torques τ_1 and τ_2 of the endoscope have to be transformed to F_z and F_y, respectively, of the Falcon as seen in Fig. 5.2, and the coordinates of the Falcon have to be transformed in the correct angles of the two joints of the endoscope's tip.

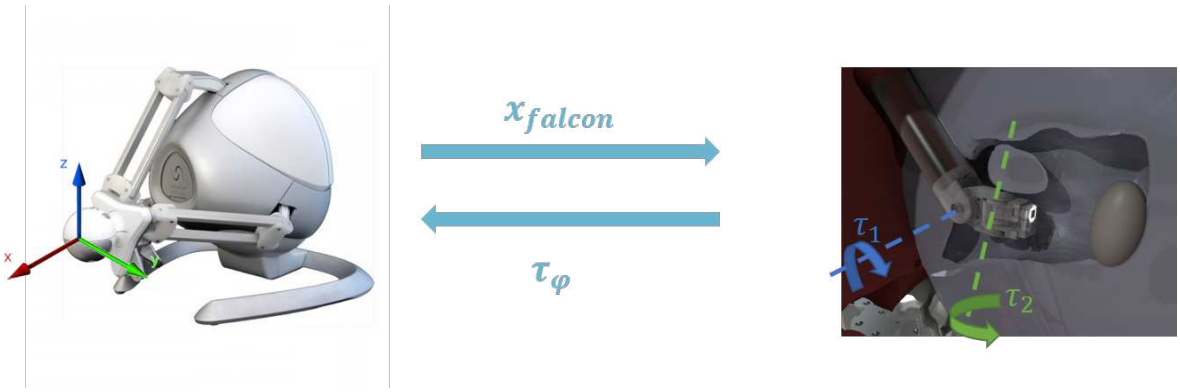

Figure 5.2: Correspondence between torques of the tip and forces of the falcon. (a) Zoom on endoscope tip with 2-DOFs, (b) Falcon haptic input device with axis.

Developing algorithms for mapping force data from sensors to haptic feedback devices is critical in creating an effective haptic feedback system, especially in applications like robotic surgery. This process ensures that the forces experienced by the user through haptic feedback accurately represent the forces applied at the endoscope tip. The process of force and position mapping can be schematized as follows;

- Data Acquisition: the first step is to collect force data from the endoscope. A Simulink code block on Twin CAT calculates and processes the deflection of the springs in the endoscope motor to find the torques applied at the tip in the two degrees of freedom.

- Force Mapping Algorithms: the core of force mapping is the development of algorithms that transform the acquired force data into commands for the Falcon. These

algorithms aim to recreate the sensation of the force for the surgeon in the most realistic way possible. The algorithms must consider various factors:

  - Haptic Device Dynamics: understanding the dynamics and limitations of the haptic feedback device is crucial. This includes its ability to reproduce forces at different frequencies and amplitudes, which was evaluated in the previous chapters.
  - Real-time Interaction: surgical procedures require real-time interaction, so the algorithms must execute quickly with low latency. This ensures that the surgeon receives immediate and responsive haptic feedback, so the communication between the parts was changed from ADS to Real-Time UDP.
  - Force Scaling: in many cases, the force data collected from sensors may need to be scaled or adjusted to match the capabilities of the haptic feedback device. In the specific scenario for which the endoscope was initially developed, brain surgery, the forces are in the order of 1-2N. These low forces will have to be enhanced to ensure they are perceivable on the user's side. Furthermore, damage forces in brain surgery are extremely close to working forces, so the mapping must ensure that even slight changes can be sensed.

- Position Mapping Algorithm: The Position of the Falcon's handle has to be sent back to the endoscope, and its tip has to move accordingly; also, in this case, there will have to be a scaling factor, the position of the falcon in mm has to be transformed in degrees to be applied to the endoscope's tip.

- Testing and Validation: Thorough testing and validation of the mapping algorithms are essential to ensure that the haptic feedback system accurately replicates the forces and tactile sensations experienced during surgery. This will be done with a small user study.

These algorithms are crucial in delivering an immersive and accurate haptic experience for users, enhancing their ability to perform tasks precisely and safely.
Using the conclusions from the previous chapter as a starting point, the easiest variable to map at first is the position. First, the correct correspondence between the 2 degrees of freedom of the endoscope and the three of the falcon must be addressed. As shown in Fig. 5.2, a positive value of z corresponds to a negative value of ϕ_1, and a positive value of y corresponds to a positive value of ϕ_2. Secondly, the range of the endoscope tip is $\pm 50^\circ$, and the workspace of the falcon in which the rendering is considered appropriate is $\pm 50mm$. Given these values, the mapping is easy to make. By aligning the two zeros, the position in mm of the falcon corresponds to the same position in degrees of the tip (Fig.5.4).

$$\phi_1 = -1000z$$
$$\phi_2 = 1000y$$

It is necessary to multiply by 1000 because the position of the falcon is given in m.

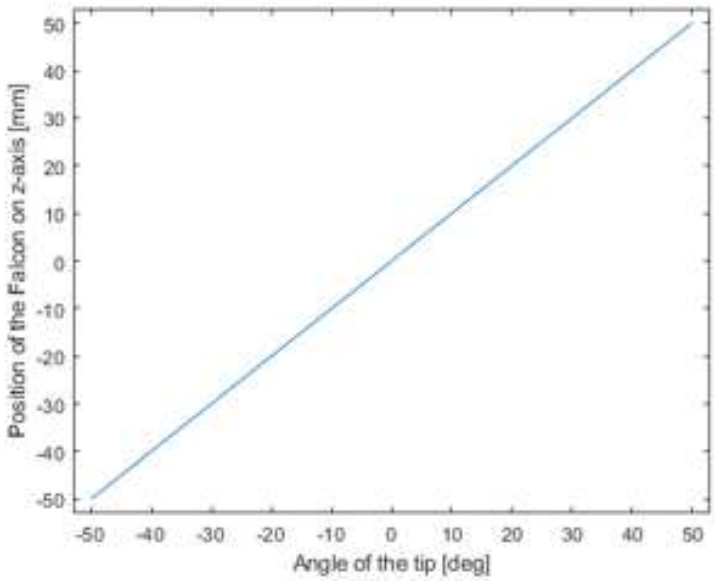

Figure 5.3: Chosen position mapping profile. Relation between the angle of the first joint of the endoscope's tip and the position of the Falcon's handle.

The force mapping is more complicated since it depends on the stiffness of the tissue we want to inspect and its limiting forces.
The most important thing to consider is making sure that the forces we want to feel are, after the mapping, still in the range in which the Falcon's rendering is reliable. To ensure the Falcon could render all the forces of interest for the specific user study, the following had to be taken into consideration:

- limited range of forces correctly rendered by the Falcon,
- specific goal of the tests,
- maximum torques that the endoscope can apply,
- internal friction of the endoscope.

It is necessary to find an adequate correspondence between the torques generated in the specific scenario and the consequent forces we want to render to use the whole range of forces that the Falcon can render correctly. By testing the setup, it was obvious that with the silicone that will be used for the user study, the kind of test we wanted to carry out, and

the internal friction of the endoscope, a linear relation between torque and force was not applicable. The relation had to be of the type:

$$Force = gain(torque) \times torque \tag{5.1}$$

Resulting in a squared dependence of the Force from the torque. Adding the squared term made it possible to minimize the effect of the internal friction of the endoscope. Furthermore, it made it possible to have a better distribution of the values in the entirety of the range of the Falcon, especially to enhance the higher and lower ones to distinguish different stiffness better.
Having decided the type of function for the relation between force and torque, the gain had to be assigned. Again, to ensure that the whole range of the Falcon was used, the gain had to be a function of the torque: $g(\tau)$. The function that best fitted the values was linear.
The first step in identifying the correct mapping is determining the torques' lower and upper limits. The τ_{min} was calculated by freely moving the endoscope tip with no kind of contact; the idea is that all torques which are registered in this scenario are caused by the internal friction of the endoscope itself and, thus, should not be felt by the surgeon. On the other hand, τ_{max} is the maximum torque that the endoscope can generate, thus imposing a threshold at which the torque saturates and no distinction is possible. The endoscope was put on the condition of hard contact to measure the upper limit. The following values were obtained:

- No contact: $\tau_{min} = 1.5 \times 10^{-3} Nm$,
- Hard contact: $\tau_{max} = 5.5 \times 10^{-3} Nm$

Given these values and the values found in Chap. 4 the actual mapping relation could be found easily from Eq.5.1 knowing that:

$$\begin{cases} \tau = 1.5 \times 10^{-3} Nm \Rightarrow F = 1N \\ \tau = 5.5 \times 10^{-3} Nm \Rightarrow F = 11N \end{cases}$$

And that the relation between gain and torque is linear:

$$gain = 3.333 \times 10^{5} |\tau| + 166.667; \tag{5.2}$$

The absolute value ensures the mapping curve is symmetric to 0. This specific gain was found by fitting a linear curve given the experimental values for minimum and maximum torque and range of forces in which the falcon performed correctly.
For $\tau \leq 1 \times 10^{-3} Nm$, the force to apply at the Falcon is imposed at zero to filter out the internal friction of the endoscope. In Fig. 5.4, the used profile is shown.

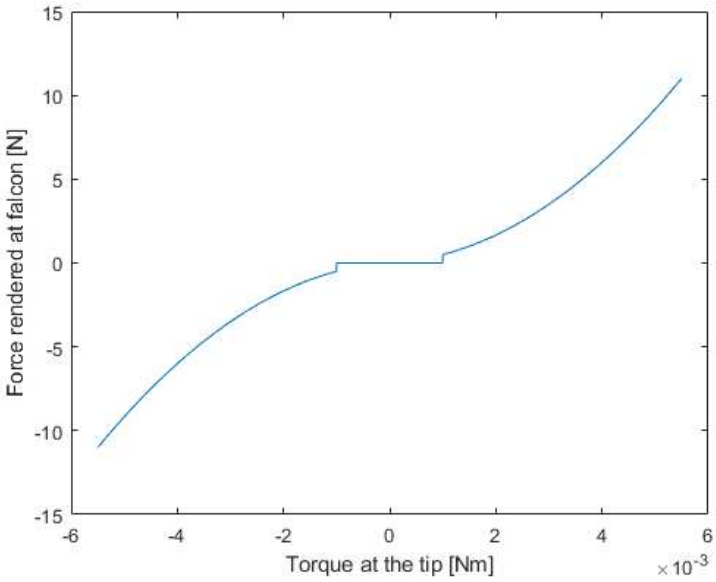

Figure 5.4: chosen mapping profile. Relation between the torque generated at the tip and force sent to the Falcon to be rendered. The discontinuity doesn't create any instability; it is meant so that there are forces at really low torques.

The discontinuity ensures that even the contact with soft surfaces creates perceivable forces; important to note is that it doesn't create any instability in the control. Furthermore, as found out in Chap. 4 the Falcons rendering is considered correct for $F > 1.2N$. Creating a function with no discontinuity could be an improvement to the mapping. It is believed, though, the most important thing is that the whole range of forces is used and that the torque caused by the friction not perceivable from the user since it could be mistaken for contact with a soft surface. The mapping we used is independent of the type of tissue used and depends only on the dynamics of the endoscope. It was observed that by slightly changing the position on the zero of the internal spring on the endoscope's control, the internal friction could change slightly, thus having to change the τ_{min}. If the silicone is swapped for a different tissue or, in a final scenario, for in-vitro brain tissue [62, 63], the force mapping could change slightly to adapt to different stiffness. Nevertheless, the chosen silicon had similar mechanic characteristics to the brain tissue and was a good starting point to evaluate the haptic feedback control [64]. The position mapping, on the other hand, depends on the dynamics of the Falcon and the endoscope tip, so if neither of them is changed, it should not need any further correction.

5.3 Experimental setup

The setup used for the user study (Fig. 5.1) is partially similar to the one described in Chap.3, but with a substantial difference at the following robot side:

- Endoscope: 2-DOF cable-driven endoscope permits the torque calculation at the tip using SEA 5.5. For the exact calculations and concept refer to Chap.2 and paper [5]

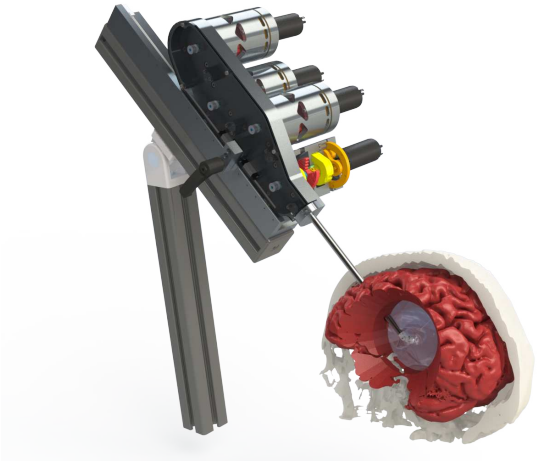

Figure 5.5: Overview of the whole endoscope. [5]

- Silicon sample: Silicon (Ecoflex 00-20 mixed at a ratio of 4:1 with Slacker to soften it to obtain Ecoflex 00-50 [64]) was poured on the plastic mold from a high altitude and slowly to prevent the creation of air bubbles in the sample. The mold is 40 mm x 40 mm x 15 mm in size, and it presents 5 square columns of size 7 mm x 7 mm x 13 mm that will create holes in the sample; these holes will then be filled with plastic insertions of the same size to achieve different stiffness in the same sample. There are eight designated contact areas between the endoscope and the sample, all will be covered with a black marker to ensure it's impossible to see the plastic insertion. The sample was then covered in plastic film to make it easy to slide down the sample holder and reach each position smoothly and quickly. The mold was designed on SolidWorks and then 3D printed in ABS, same for the plastic insertions.

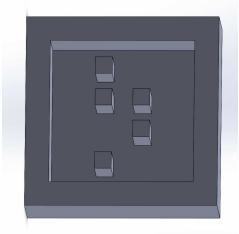

Figure 5.6: Solidworks CAD of one of the sample molds.

- Sample holder: a sample holder was designed on SolidWorks to attach and stabilize the sample to the articulated arm. It was fixed at a 45° angle, making it parallel to the endoscope shaft. On the side of the holder, three holes were placed to add screws to block the sample from falling out while, at the same time, keeping it in the four different positions required for the investigations,

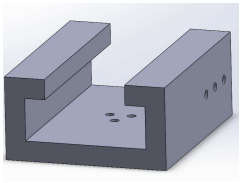

Figure 5.7: Solidworks CAD of Sample holder, with holes for the attachment to the force sensor on the bottom, and holes for the position holding of the sample on the side.

- Webcam: it was mounted on the shaft of the endoscope, and it showed the exact contact point between endoscope's tip and sample in order to also give visual feedback during the test and make it as similar to a real procedure as possible; the camera was mounted on the shaft with adaptors,

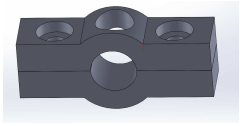

Figure 5.8: Solidworks CAD of adapter to attach the Webcam to the endoscope shaft.

- Three degrees of freedom adjustable articulated arm, Force/torque sensor, and adaptor were the same as described in Chap.3.

The user controlled manually the Falcon connected via USB cable to the PC, which is connected via UDP to the Real-Time PC. On the surgical side, the endoscope is controlled by a Simulink code on the real-time PC. The silicone sample is placed at the correct height using the three-degrees-of-freedom adjustable articulated arm; we placed the force torque sensor between the two. Furthermore, on the endoscope, we placed a webcam to give visual feedback to the user with a surgery-like perspective.
On the PC, a C++ code received torque information via UDP and, by applying the mapping in Eq. (5.2), transformed it into forces to apply to the Falcon. At the same time, the code read the position of the Falcon and sent it to the real-time PC. As a safety feature, a force different from zero was calculated and applied only if the central button on the handle of the falcon was pressed. By pressing and releasing the button, a clock was also respectively started and stopped; this will then tell us the time required from the user to do each inspection. The

necessity to keep the button pressed is not only given by the previously mentioned reasons but also to make sure that the system is more stable; indeed, as stated in [65, 66], the human presence and handling of the haptic device stabilizes the whole system. Furthermore, by pressing a button, a counter was set to send an increasing step for each position, making data extraction and further analysis more automatic. The data was sent back and forth between the two computers at a rate of 1kHz.
On the real-time PC, Twin-CAT was running, at a rate of 1kHz, the whole control of the endoscope and, at the same time, a PLC code used to receive and send data via UDP. The same PLC code was used to detect the forces being applied on the sample, using the force torque sensor as in Chap.3.

5.4 Study procedure

In Fig. 5.9 the whole setup used for the user study is shown, focusing mainly on the endoscope and on the silicone sample.

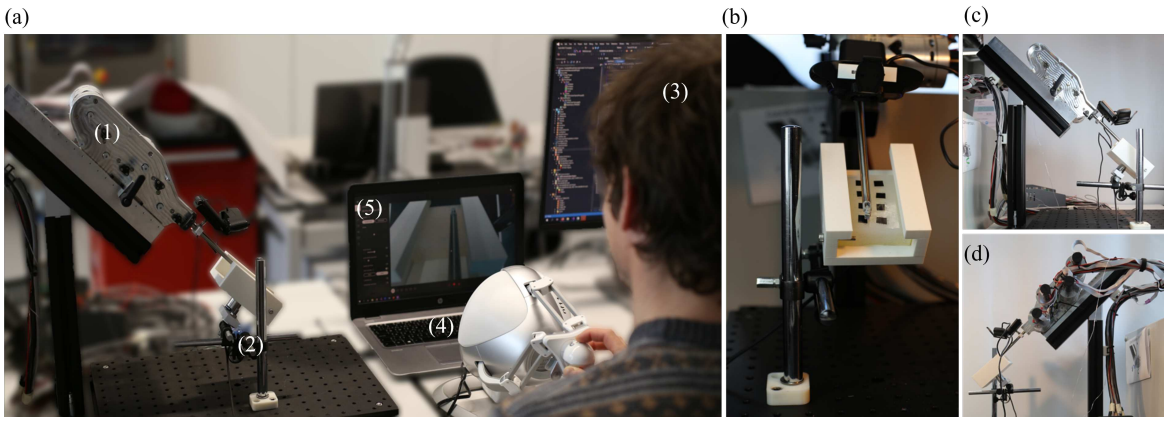

Figure 5.9: (a) User doing the test: (1) endoscope with webcam, (2) sample with sample holder and force sensor, (3) user doing the test, (4) haptic input device, Falcon (5) PC with visualization of endoscope tip; (b) front view of sample and endoscope's shaft; (c) and (d) side views of endoscope + sample whole set up

The user study was divided into three sections, followed by a questionnaire. The user will receive visual feedback on the endoscope tip in all investigations. The three samples used in the investigations have insertions in different positions to make the inspection as unbiased as possible.

- Investigation number 1: the user is only asked to say if the position n on the sample (a) of Fig. 5.10 is harder or softer than the previous one. This first test is used to get the user acquainted with the system. Furthermore, since the single user's learning curve

has to be taken into account, we hypothesize that the big ”jump” in knowledge takes place during this first investigation. (TEST)

- Investigation number 2: The user in this test will be asked, having only visual feedback, if each site of contact of the sample (b) of Fig. 5.10 is hard or soft (noHF: no haptic feedback).
- Investigation number 3: The user in this test will be asked, having both visual and haptic feedback, if each site of contact of the sample (c) of Fig. 5.10 is hard or soft (HF: haptic feedback).

Figure 5.10: Samples used for the three investigations. The tick marks the presence of the plastic insertion. (a) test to get acquainted, (b) noHF, (c) HF.

Furthermore, to try and lower as much as possible the influence that the learning curve of the single user had on the overall results, investigation number 2 and investigation number 3 were not given to all users in the same order; in other words, half of the users did the test with haptic feedback before the one without haptic feedback and the other half the opposite. Since the endoscope tip was fixed, the sample had to be moved by hand between inspections to move from one position to the next. To ensure that the positions were the same in every scenario, appropriate marks were placed on the sample holder. The time it took to manually move the sample was not considered, and instead only the actual palpation time was recorded.
During the test, the user was asked to start the inspection by pushing the button and releasing it when they felt confident to make a decision about the tissue's stiffness. There was no time limit for each inspection, and the user was asked to move relatively slowly to avoid instability. Since during surgery the movements are slow and at low frequencies we don't considered the request to be a limiting or altering factor for the correct comprehension of the results. In the endoscope torque control a torque limit is imposed at $5.5 \times 10^{-}3\,Nm$ to avoid getting in an error state or applying high forces. A Speed limit was also imposed at $40^{\circ}/s$.
To get an idea of the confidence level, the users were asked how many they thought they managed to get right after each investigation. At the end of all three inspections, the users were asked to reply to the following list of questions:
Question 1: Did the force rendering feel natural? (scale from 1 to 5)
Question 2: Do you think it took you more or less time than with the haptic feedback?
Question 3: Do you think you exerted higher forces with or without the feedback?

To try and evaluate if the added feature of haptic feedback was useful for the user, the following metrics were measured:

- Success/failure in the detection of the stiffness,
- Average and maximum torques of the tip,
- Average and maximum forces detected from the sensor,
- Time required,
- Position of the tip,
- Answers to the questionnaire.

A YT Scope Project was launched on Twin CAT to get said data.
The data received from the tests and the questionnaire were statistically evaluated. Even if the number of users was low, potentially limiting the statistical power, some preliminary information and conclusions could be drawn anyway, and, if positive, could be the starting point for a bigger and more in-depth user study.

5.5 Data processing

The data acquired from the force sensor during the user study has to be processed in order to extract the information we are interested in.

The force/torque sensor data was used to validate the data acquired through the endoscope control (torque and position). Also, in this case, the data that interested us was the force since no torque was applied to the sensor. To use the force data, a first supposition has to be made: since the sample holder is a rigid body, the forces applied at the point of contact can be considered the same as the ones perceived by the sensor. On the other hand, the silicone of the sample is so soft that when a deformation is applied on one of the surfaces of the sample, the deformation is perceivable also on the opposite surface; said deformation will then apply a force on the sample holder.

To compare the forces in N, coming from the sensor and the torques, in Nm, the latter has to be divided by the lever arm to obtain a force always perpendicular to the lever arm. The lever arm is defined as the distance between the center of rotation, in this case, the link, and the point of contact, in this case, the tip of the endoscope. The lever was measured to be 1cm. Thus, the torques had to be multiplied by 100 to obtain force measurements. The sample, along with the sample holder and the force sensor attached to it, are set at a position of 45 °in order to make them parallel to the endoscope's shaft. When the endoscope's tip is in its zero position the z-axis of the sensor and the endoscope are perpendicular. The forces applied to the sample by the endoscope are assumed to be always perpendicular to the tip; in other

words, the only forces that we assume are applied are the ones equal to $\frac{\tau}{l}$.
The sensor gives the force information along the three axes as an output. Assuming $f_y = 0$, the total force is $|f_{tot}| = \sqrt{(f_x)^2 + f_z^2}$, in the range of interest the direction of these two components is the same and always negative resulting in a total negative force in the sensor's reference system, see Fig. 5.11.

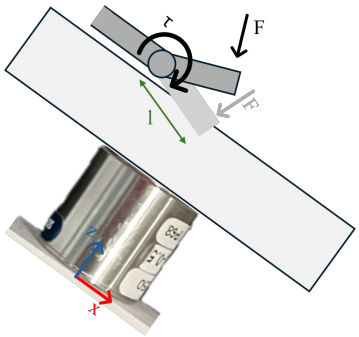

Figure 5.11: Schematic side view of the setup: sensor, sample, and endoscope tip. F is the force applied by the tip on the sample always perpendicular to the tip; l is the lever arm, τ the torque around the first joint. On the sensor is also reported its reference system

6 Results and Discussion: User study

For the overall comprehension of the results and a correct and objective evaluation, it has to be taken into account that the test is extremely sensible to the user's personal perception, a reason which is probably the use of surgeons who are specialized in tissue stiffness detection, could give different, more complete and more relevant results.
The data was exported from TwinCAT to MATLAB as .cvs files to start the data analysis. Each investigation was loaded as an independent file to make the division easier. In MATLAB, only the data recorded during the inspections was extracted and used for the analysis. The following values were computed:

- average and maximum torques for each position for each user,
- average and maximum forces for each position and each user,
- time required for each inspection for each user,

It was decided to group the data for each participant to have 8 data points for the 10 participants. In the plots in the following chapter, each data point represents a different user.

6.1 Success rate

The success rate was high for both scenarios, with and without haptic feedback. Out of 80 total inspections, 8 per user for 10 users, six mistakes were made without haptic feedback, success rate of 92.5%, and only four with, success rate of 95%. This difference can not give us any statistical evidence that using haptic feedback is useful. Still, we can already observe that the delays, even if high as calculated in Chap.4, do not seem to affect the user's experience, altering their perception.
The most common mistake was the perception of a hard tissue as soft; this could be caused when using haptic feedback by the delay, which, as previously stated, when coupled with visual feedback, could cause the user to perceive a softer material.
For the table of results, refer to Appendix C.

6.2 Stability and Transparency

When dealing with haptic feedback in surgery, the trade-off between transparency and stability is of utmost importance (Chap. 2). These two characteristics make telemanipulation realistic and haptic feedback useful. The telemanipulation's transparency resulted from the mapping (Chap. 5). To ensure stability in the system, a speed limit was imposed on the endoscope tip to avoid any unwanted fast jumps in the torque, especially when dealing with hard contact. With the choices made, the whole system remained stable in the range of speed and forces considered useful for brain surgery, even when dealing with hard contact. The transparency and the stability were evaluated by asking the user to score, on a scale from 1 to 5, the experience. Out of the ten users, 8 evaluated it with a score of 4/5, one with a 3/5, and one with a 5/5. When asked what was lacking or what could have been better, all stated there was a significant delay in the camera, which made the telemanipulation confusing, especially when having two input information like in the case with haptic feedback.
A second metric to evaluate the transparency-stability trade-off was asking the user, for each of the two scenarios, how many positions out of 8 they thought they had correctly determined. The overall trend is higher confidence with the use of haptic feedback, suggesting that the whole control felt natural and easy to use. It is also interesting to note that, in general, the user was pessimistic about the score; the user's lack of training and the system's novelty could cause this.

Integrating the second degree (Fig.6.1) of freedom in the control is a limiting factor for the system's stability. The longer tendon routing adds friction in the transmission, which lowers the limit at which the torque saturates, making it impossible to differentiate different stiffness. At the same time it elevates the torque caused solely by friction, since now two joints and 4 tendons have to be taken into account. As a result, the range of torques that are applicable for force feedback is extremely low, and it was seen that only the force required to apply slight pressure on the soft tissue already saturated the torque. These aspects made the system unstable, especially when getting out of contact with the surface, and it was hard to detect the difference between the two tissues. Since, for this user study, only one degree of freedom was evaluated, this problem was solved by eliminating the influence of said second degree of freedom. Still, it must be addressed if a complete evaluation is necessary. An idea to solve this problem could be to higher the maximum torque, that could mean though that some design changes in the tip itself are needed, as much as changing its material.

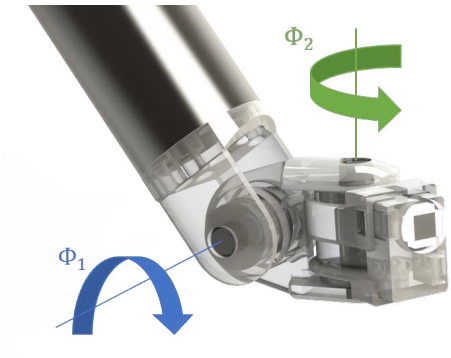

Figure 6.1: Zoom on the endoscope's tip with a highlight on the two degrees of freedom. In blue is the first one, the one being evaluated with the study, and in green is the second. [5]

6.3 Time and Torque

The first step was to determine if the data acquired and on which the consideration had to be made were normal because it changes the test that can be carried out on the data set. To do so, a specific function [67] was downloaded along with the specific toolbox. The following data passed the Shapiro-Wilks test for normality [68] with a tolerance of $\alpha = 5\%$:

- Time required, averaged per user, with and without haptic feedback separately,
- average torque with and without haptic feedback separately

On the other hand, the maximum torque registered for each inspection did not pass the test for normality, probably because in both scenarios, most of the inspections when dealing with hard tissues reached the maximum torque $\tau_{sat} = 5 \times 10^{-3} Nm$, making the distribution non-normal.
The paired student's t-test for two populations with a tolerance of $\alpha = 5\%$ was carried out for the paired duration data set. This test evaluates the null hypothesis and assumes that the true mean difference between the paired samples is zero; the variances were considered different. This test was used to take into consideration the strong correlation there is between these two populations and take into account the big data variability there is between one user and the other. In other words, time, much more than torques or forces, depends on the single user and their perception and experience. The hypotheses used are the following:

$$H_0 : \mu_d = 0 \qquad H_1 : \mu_d \neq 0 \qquad where \qquad \mu_d = \mu_2 - \mu_1 \tag{6.1}$$

- Population 1: Time required with haptic feedback,
  Population 2: Time required without haptic feedback.
  When the paired test was carried out for the total average of the time needed by each

participant, the null hypothesis was accepted, stating no statistically significant difference between the two populations. On the other hand, if the same test was carried out, dividing the two populations between the time required for hard surfaces and soft surfaces, the test would have refused the null hypothesis in the first case.

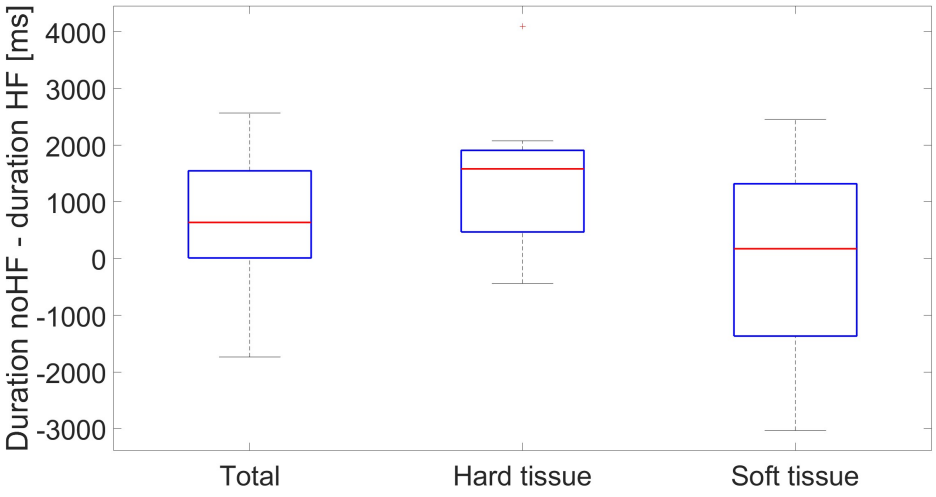

Figure 6.2: Box-plot of the difference between the two populations when considering the two tissues together(left), when considering only the hard tissue (middle), when considering only soft tissue (right). The red line is the mean for each population. Red plus signs are the outliers.

The results of the paired student's t-test are evident also by observing the box-plots in Fig. 6.2, this shows a higher facility in detecting the stiffer surfaces, than softer ones. In other words there is a statistically significant reduction in the time needed to detect the presence of a harder insertion. Furthermore, it must be noted that the data set is limited, thus complicating any statistical analysis. The users, though, when asked if it took them more or less time to decide in the two scenarios, all replied it took them less time while using haptic feedback. This shows again the higher confidence they had while doing the investigation with the added feature.

The student's t-test for two populations with a tolerance of $\alpha = 5\%$ was carried out for the paired normal data set. This test evaluates the means of two populations, the variances were considered different. The hypotheses used are the following:

$$H_0 : \mu_1 = \mu_2 \qquad H_1 : \mu_1 \neq \mu_2 \tag{6.2}$$

The test gave the following results:

- Population 1: Average torque applied by each user with haptic feedback,
  Population 2: Average torque applied by each user without haptic feedback.
  Statistical difference between the two means, rejected the null hypothesis.

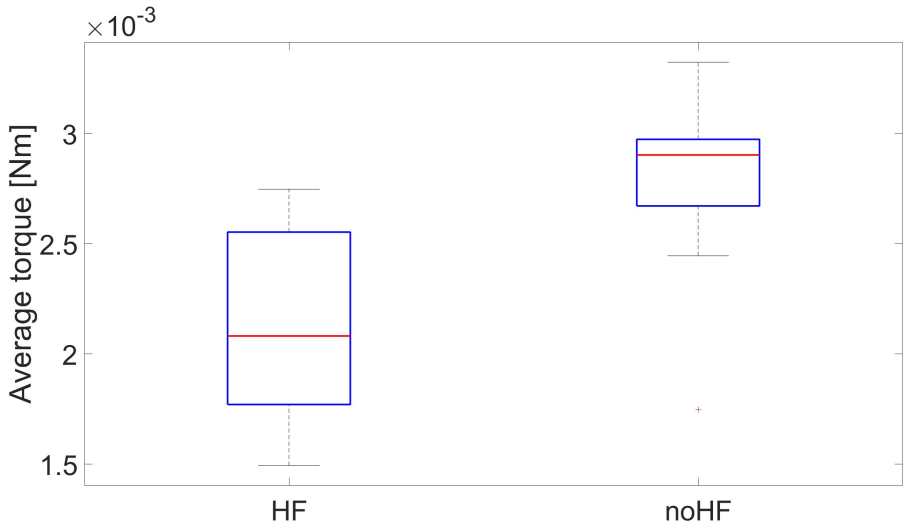

Figure 6.3: Box-plot of the average torque in the two different conditions. The red line is the mean for each population. Red plus signs are the outliers.

Fig. 6.3 shows the difference there is between the two populations. The much smaller variance in the second population could be caused again by the fact that most inspections reached the maximum torque without haptic feedback. In contrast, there was much more variability with haptic feedback, depending on the user.

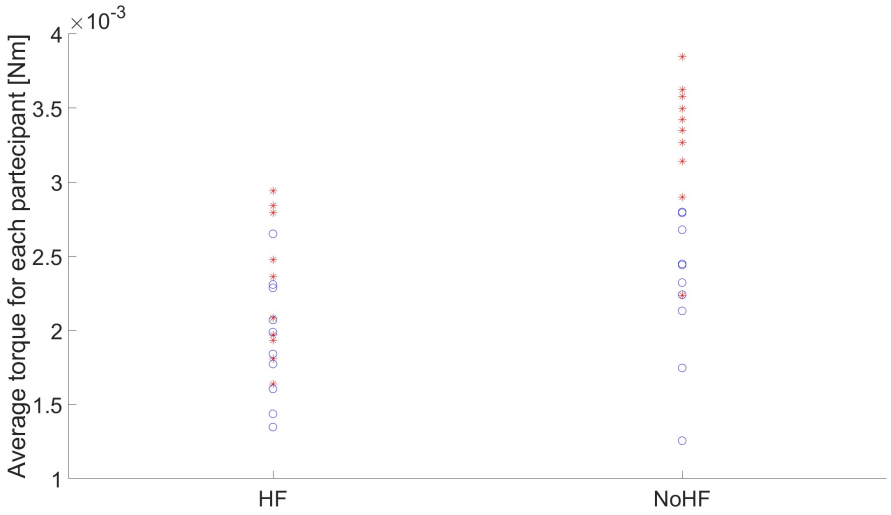

Figure 6.4: Single data points for the average torque for each participant in the two different conditions. * symbol identifies hard surfaces, °symbol identifies soft surfaces.

From Fig.6.4, it is possible to see how haptic feedback helps the user to apply lower torques, especially when dealing with harder surfaces.

For the maximum torque applied by each user, the Wilcoxon-Whitney U test for nonnormal populations was carried out. This test evaluated the median of two populations. The maximum torques for each user were calculated as:

$$\tau_{maxhard,i} = \sum_{n_{hard}=1}^{5} \tau_{max,n_{hard}} \qquad \text{and} \qquad \tau_{maxsoft,i} = \sum_{n_{soft}=1}^{3} \tau_{max,n_{soft}}$$

where i=[1,10], is the number of participants and n_{hard} is the number of hard inspections for each user and n_{soft} is the number of soft inspections for each user.
The hypotheses used are the following:

$$H_0 : median_1 = median_2 \qquad H_1 : median_1 \neq median_2 \tag{6.3}$$

The result rejects the null hypothesis, stating that the two populations have statistically different medians as shown in Fig. 6.5.

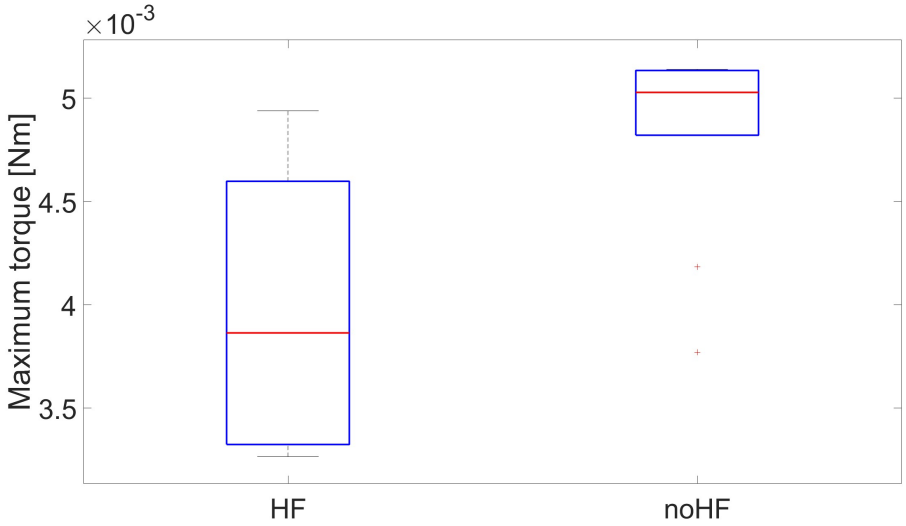

Figure 6.5: Box-plot of the maximum torque in the two different conditions. The red line is the mean for each population. Red plus signs are the outliers.

What is interesting to note for this specific measurement is the big difference, again, between the variability of the two data sets. This fact can be justified by analyzing the maximum torque without haptic feedback. Indeed, it reaches the saturation value for nearly all inspections, showing that the user has to push the endoscope to its limits to ensure the tissue's stiffness. The saturation level is reached when dealing with harder surfaces, with no haptic feedback. This is shown even more clearly in Fig. 6.6

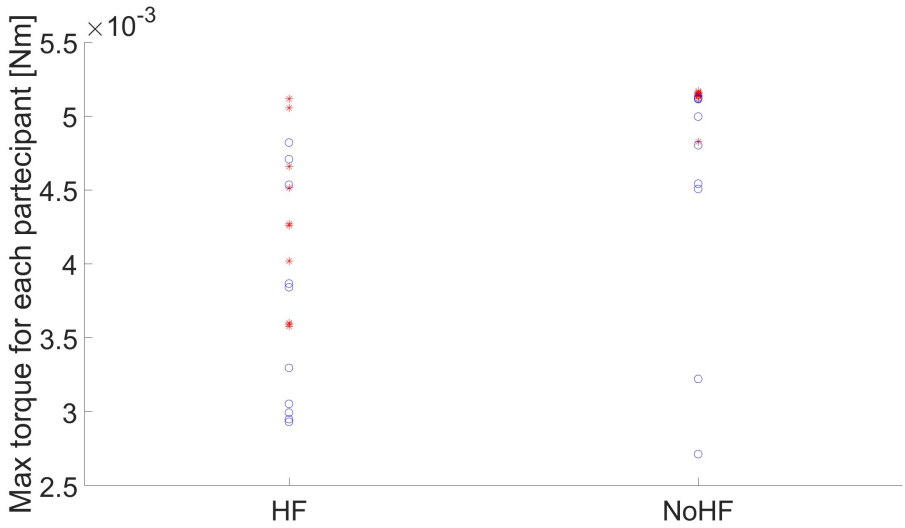

Figure 6.6: Single data points for the maximum torque for each participant in the two different conditions. * symbol identifies hard surfaces, °symbol identifies soft surfaces.

6.4 Forces

The four datasets, maximum and average force registered with and without haptic feedback, were tested for normality with the Shapiro-Wilks test, as in the previous paragraph. As for the torque, the average forces passed the test, while the maximum did not. The mean of the two normal populations and the medians of the two nonnormal ones were tested with the same tests as for the torque. Both cases brought about the refusal of the null hypothesis, thus stating a statistical difference between the means and the medians. The test results are also shown with the box-plots in Fig.6.7 and Fig.6.8. For the maximum forces the same calculations made for the maximum torque were carried out.

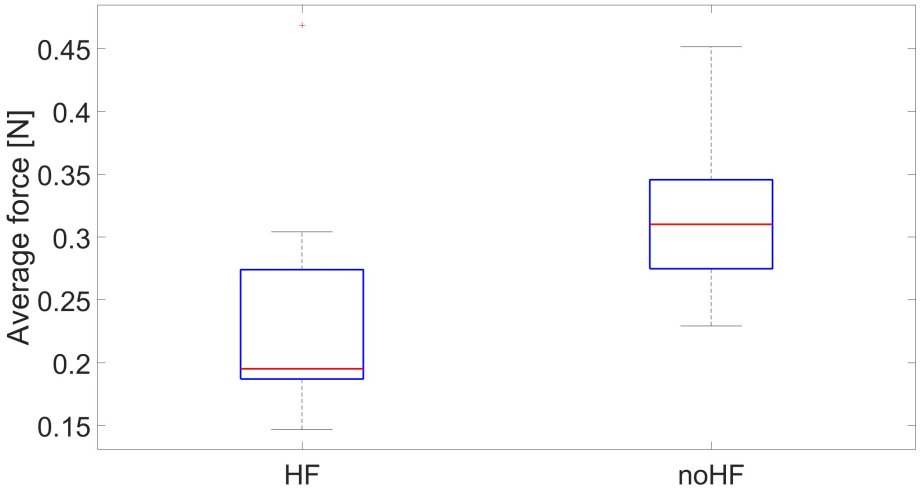

Figure 6.7: Box-plot of the Average force in the two different conditions. The red line is the mean for each population.

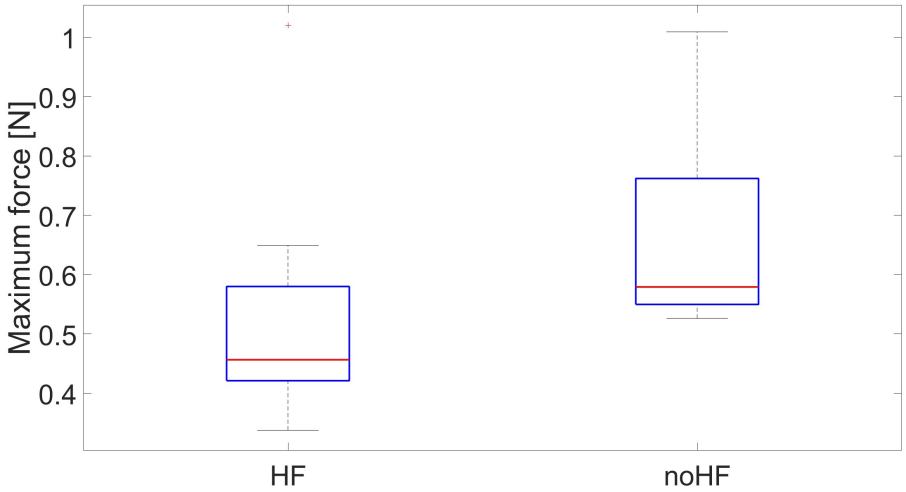

Figure 6.8: Box-plot of the maximum force in the two different conditions. The red line is the mean for each population. Red plus signs are the outliers.

After adjusting the two measurements as explained in 5 to make sure we were comparing two similar quantities, the student's t-test was carried out on the average force collected from the sensor (F_{sensor})and the one calculated from the torque($F_{SEA} = \frac{\tau}{l}$), giving the acceptance of the null hypothesis, see Fig.6.9. This result confirms that using the sensor as a golden standard and a reference point, the torque information received from the endoscope and sent to the Falcon for haptic feedback is indeed the force that is being applied at the surgical site.

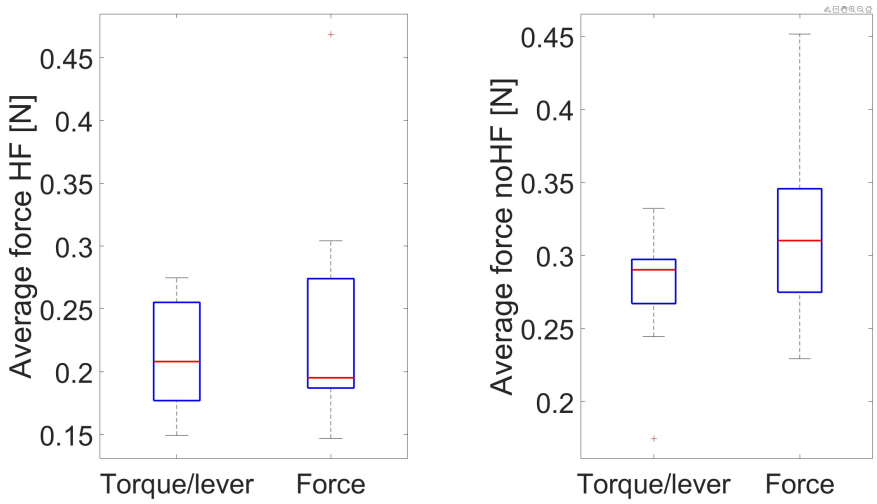

Figure 6.9: Box-plot of the F_{SEA} and F_{sensor} . (a) Test with haptic feedback, (b) test without haptic feedback. The red line is the mean for each population. Red plus signs are the outliers.

As shown in the following two plots in Fig. 6.10, we can see that not only does the sensor follow the torque for the most part, but actually, the torque data has less noise, especially when reaching saturation. The total average error between the two signals is of -0.0249 N, indicating that in general the force sensor measures higher values than the ones calculated through the torque data. The force data does not follow the torque data when the torque is negative because there is no contact in that scenario, and the residual torque is due to the internal friction of the endoscope.

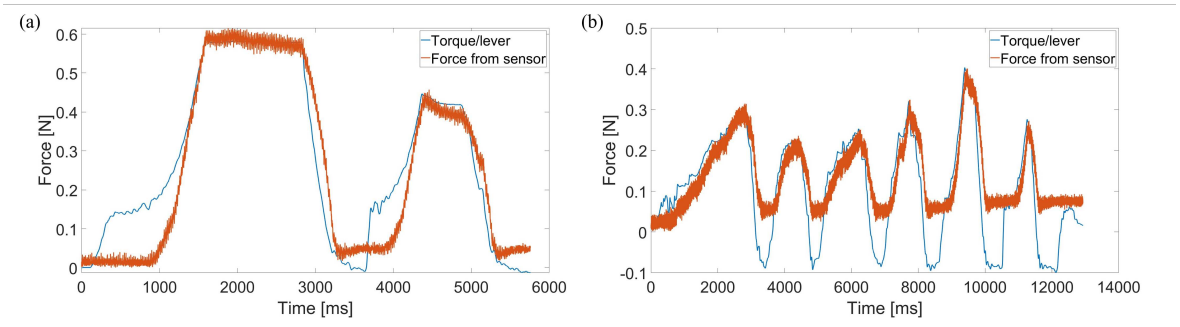

Figure 6.10: Profile of the $F = \frac{\tau}{l}$ and the force from the sensor from user number 6. (a) Hard tissue contact, (b) soft tissue contact.

One last consideration regarding the forces can be made by looking at the values. Indeed, they remain under the limits of damaging forces (2N) in brain surgery found in literature and reported in Tab. 2.1.

6.5 Position

In brain surgery, high-impact forces could cause lacerations in the tissue, and applying too much deformation to said tissue could cause serious problems. Thus, it is important to see how much the user had to deform the tissue to make a decision in the two scenarios. We expect the user to apply a higher deformation to the tissue in the scenario without haptic feedback since it had to rely solely on the camera focusing on the contact point. As predicted, there is a difference between the two scenarios and between hard and soft tissue, as shown in Fig.6.11. In particular it is possible to note that when using haptic feedback the user was able to detect soft surfaces applying a much lower deformation to the tissue, this is also seen in Fig. 6.12. The results are reported in Tab.2.1.

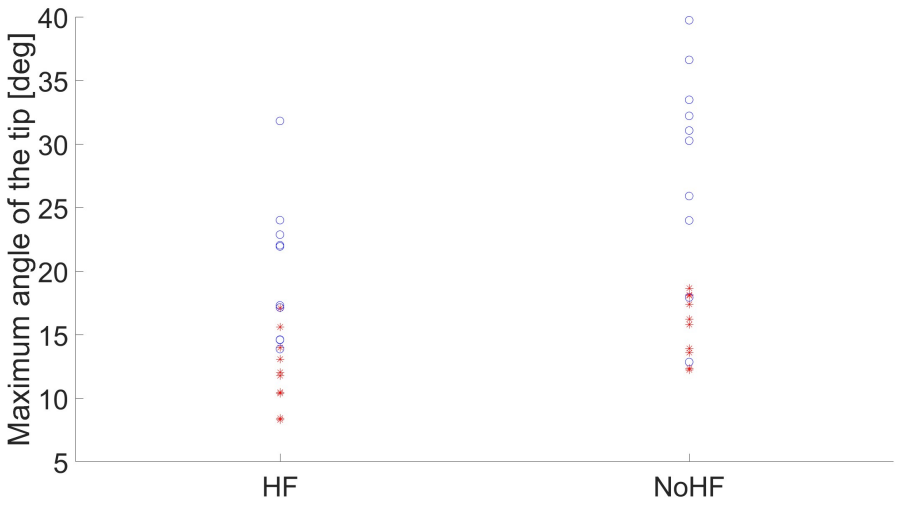

Figure 6.11: Single data points for the maximum angle of the endoscope's tip for each participant in the two different conditions. * symbol identifies hard surfaces, °symbol identifies soft surfaces

In Fig.6.12, it is possible to see how, it is really easy to distinguish hard and soft surfaces and how the torque in the scenario without haptic feedback always reaches saturation. The tip angle without haptic feedback reaches values very close to the endoscope's position limit of 50°when dealing with soft tissues. After that, the tip does not follow the haptic input device, making telemanipulation more complicated and counterintuitive. On the other hand, with haptic feedback, the user could already make decisions at lower joint deflection angles, thus lowering the risk of damages. When inspecting hard tissues the angle of the joint is the same in the two conditions since it is physically blocked by the tissue itself, On the other hand though we can appreciate how the torque does not always reach saturation as in (b) of Fig.6.12.

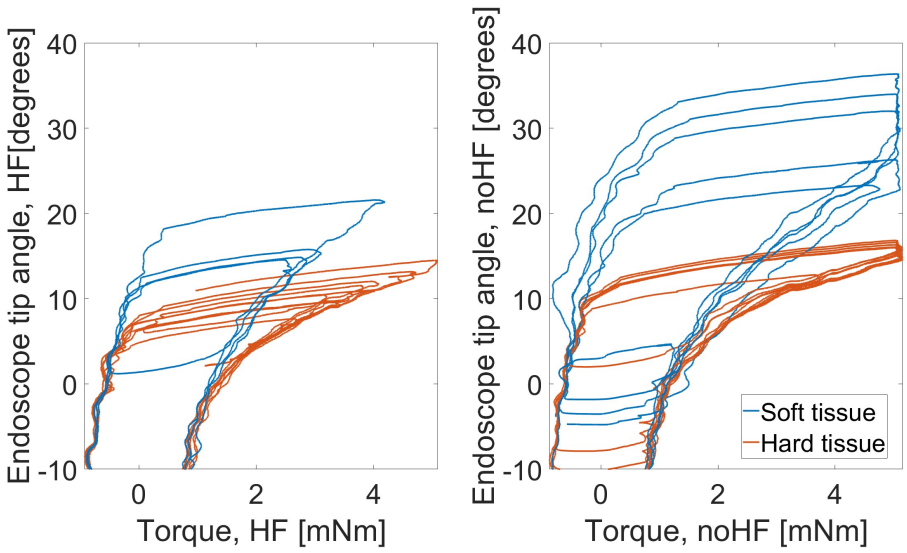

Figure 6.12: Profile of the angle of the endoscope's tip referred to the torque around the first joint in the two different conditions. (a) Inspection with haptic feedback, (b) inspection without haptic feedback. Blue lines $\rightarrow$ $softtissues, orangelines \rightarrow hardtissue. The two figures plot the values for user number 6.$

6.6 Summary and Limitations

In Table 6.1 all values are summed up in the following way: $\mu \pm \sigma$

	Maximum Torque [mNm]	Average Torque [mNm]	Maximum Force [N]	Average Force [N]	Duration [ms]	Maximum Angle [deg]	Avegare Angle [deg]
Hard Tissue	4.3 ± 0.7158	2.3 ± 0.575	0.56 ± 0.2993	0.26 ± 0.1539	4202.4 ± 2506.3	12.1161 ± 2.9750	8.4547 ± 2.7763
	5.1 ± 0.1716	3.3 ± 0.4967	0.5963 ± 0.0706	0.319 ± 0.0706	5593.6 ± 2533.3	15.6349 ± 2.3949	12.2578 ± 2.4535
Soft Tissue	3.7 ± 0.8432	1.9 ± 0.4769	0.3601 ± 0.1090	0.2118 ± 0.1985	4498.4 ± 2756.7	20.0144 ± 5.9143	13.2862 ± 4.5650
	4.5 ± 0.9152	2.3 ± 0.5896	0.7334 ± 0.4884	0.3248 ± 0.1968	4508.3 ± 2251.6	28.3999 ± 9.0759	17.6922 ± 5.9023

Table 6.1: Table of all the values previously described divided into hard surface (first to rows), and soft surface (rows 3 and 4), and divided into hard surface (dark gray rows) and soft surface (light gray rows). The values of the Torque are the ones estimated with the endoscope, while the values of Force are the ones measured by the sensor.

The data were averaged over each user and then across all users. The results of the pilot user study suggest that haptic feedback allows the inexperienced user to accomplish the same task with lower torques in a shorter time and in a less invasive way. The implemented haptic feedback control coupled with the novel endoscope could bring great advantages to robotic surgery.

The following aspects were found to be limitations for this user study and would have to be addressed and researched further:

- The quality of the video was considered to be too poor. The image was delayed in comparison to the actual movement, confusing the user. a possible solution could be to use higher-quality cameras,

- The number of users and thus of data points, was low, making it difficult to do significant statistical analysis,

- The reply to each inspection was binary, hard or soft, making it maybe too easy for the user to guess the correct answer. A possible solution could be using more than two samples with different stiffness.

6.7 Future works

This thesis provides a promising foundation for developing a stable haptic feedback control, holding promise for more realistic and safe teleoperations using the SEA-based endoscope. However, further validation and research are still needed. An expansive user study is needed for future developments, including a larger number of users and a broader spectrum of participants ranging from novices to experienced surgeons. Diversifying the participant pool and tasks to complete ensures a more robust validation of the attained results. Moreover, involving experts brings forth insights into the practical applicability of the haptic feedback system within real-world surgical practice.

Furthermore, considering potential enhancements or alterations in the hardware, especially the leader-side robot, constitutes a promising avenue for advancing the system's capabilities. By using a different haptic input device, the range of forces correctly rendered could be broader, and by using hardware specifically built for surgical telemanipulation, latency could be lowered significantly.
Different alternatives could be tested to validate the choice of the mapping (e.g., linear mapping, higher starting point force) and cross-referenced to see which fits the needs of the specific task best.
Integrating the second degree of freedom of the endoscope tip in the control causes problems with stability due to its internal added friction, which must be addressed to make a more complete evaluation of the system.
Finally, the user study could be carried out using in-vitro brain tissue to ensure that the previously validated mapping and hardware fit all the specific requirements set by the real tissue and its softness correctly. The use of brain tissue could also be interesting to see if it is possible to detect the small difference between palpating the tissue and damaging it, while also being able, with the same mapping algorithm, to detect hard tissues, such as tumors.

Furthermore, tumors in the brain can be spread out structures, possibly really soft, and could not be simulated by a single insertion, as in this study.

7 Conclusions

In telemanipulated robot-assisted minimally invasive surgery, the leader and follower robots are completely decoupled. The big void is the absence of haptic feedback, making it difficult for the surgeon to feel anything happening at the surgical site. Inserting the feature of touch is challenging because of many complications caused by hardware (e.g. biocompatibility and cost of devices) and software (e.g. stable and transparent control). This thesis aims to tackle this issue head-on, starting with the SEA-based endoscope as a foundation. This specialized endoscopic tool reduces contact forces and provides crucial torque data, offering insights into the forces required to manipulate the endoscope's tip at various angles. Leveraging this data, the aim is to provide users manipulating the leader robot with kinesthetic force feedback.

The first step involved implementing a UDP communication protocol to transmit the torque data between the leader and follower robots. Delays of only a couple of milliseconds were detected for each round trip time, confirming the choice of communication protocol for this application. Furthermore, no significant data loss was witnessed.

The chosen leader robot is the Novint Falcon, which was evaluated concerning force rendering limits and latency. It showed that even if not ideal for brain surgery, the chosen robot could be a good, easy to access on the market, and cheap possibility. Both the internal friction of the device and its actual threshold limited the range of reliable force rendering [2N-10N]. A limitation is the time delay between the commanded signal and the rendered force, exceeding the limits in the literature of around 50ms.

The development of a robust mapping algorithm is central to integrating haptic feedback. The algorithm accounts for the constraints of the Falcon and endoscope control systems, resulting in transparent and stable force feedback. Furthermore, a small-scale user study validated the effectiveness of the mapping algorithm and haptic feedback system. This study aims to determine the benefits of combining haptic and visual feedback during palpation and stiffness recognition tasks. As discussed in Chapter 6, the results show promising outcomes, indicating reductions in both time and torque exertion when adding haptic feedback.

In conclusion, this work lays the groundwork for further exploration and refinement of haptic feedback integration in robot-assisted micro-invasive surgery with the SEA-based endoscope. Even if the actual relevance in a real-world scenario would have to be investigated further, this thesis highlights the potential that the implemented haptic feedback holds in enhancing surgical precision and efficiency.

A Appendix A

In the following appendix some important lines of the code used to send and receive data are reported.

Listing A.1: C++ code used on PC Opening of the UDP socket and generate remote and local addresses

```
//UDP

//initialization Winsock library
WSADATA wsaData;
if (WSAStartup(MAKEWORD(2, 2), &wsaData) != 0) {
    std::cerr << "Error in the initialization of Winsock." << std::endl;
    return 1;
}

//create UDP socket
SOCKET udpSocket = socket(AF_INET, SOCK_DGRAM, 0);
if (udpSocket == INVALID_SOCKET) {
    std::cerr << "Error in the creation of UDP socket." << std::endl;
    WSACleanup();
    return 1;
}


//FLEXENDOCAB = remote
sockaddr_in RemoteAddress;
RemoteAddress.sin_family = AF_INET;
RemoteAddress.sin_port = htons(10000); // remote server poort
RemoteAddress.sin_addr.S_un.S_addr = INADDR_NONE; // initialize
```

```
//PC = local
 sockaddr_in LocalAddress;
 LocalAddress.sin_family = AF_INET;
 LocalAddress.sin_port = htons(11000); // local server poort
 LocalAddress.sin_addr.S_un.S_addr = INADDR_NONE; // initialize

 // resolve remote IP adress manually
 if (inet_pton(AF_INET, "169.254.1.1", &(RemoteAddress.sin_addr)) <= 0) {
     std::cerr << "Error in the resolution of the IP address." << std::endl;
     // closesocket(udpSocket);
     // WSACleanup();
     return 1;
 }
 // resolve local IP adress manually
 if (inet_pton(AF_INET, "169.254.3.1", &(LocalAddress.sin_addr)) <= 0) {
     std::cerr << "Error in the resolution of the IP address." << std::endl;
     // closesocket(udpSocket);
     // WSACleanup();
     return 1;
 }

 bind(udpSocket, (struct sockaddr*)&LocalAddress, sizeof(LocalAddress));
```

Listing A.2: C++ code used on PC to get information from falcon and sending it via UDP

```
// HAPTIC LOOP
while (!done) {

    t1 = dhdGetTime();
    if ((t1 - t0) > REFRESH_INTERVAL) {

        // retrieve information to display
        freq = dhdGetComFreq();
        t0 = t1;



       int RemoteAddressSize = sizeof(RemoteAddress);

        //get position from the falcon:
        dhdGetPosition(&px, &py, &pz);

        if (pz > 0.05 || pz < -0.05) { // limit the workspace
        //between 50 mm and -50 mm
            pz = (pz / abs(pz)) * 0.05;
```

```
        }

        position.a = pz;

        // std::cout << "pos: " << pz << "\n";
        int userbutton = (dhdGetButton(0));

        if (userbutton == 1 && previousbutton == 0) {

            start[i] = dhdGetTime();

            previousbutton = 1;

        }
        if (userbutton == 0 && previousbutton == 1) {

            stop[i] = dhdGetTime();

            i = i + 1;
            previousbutton = 0;

        }

        //sends increasing vlue to make sure it's easy when dealing with the data
        if (previousbutton ==1) {
            position.counter = i+1;
        }
        else {
            position.counter = 0;
        }

        //SEND data both position and counter
        int dataSend = sendto(udpSocket, reinterpret_cast<char*>(&position),
        sizeof(position), 0, (struct sockaddr*)
        &RemoteAddress, RemoteAddressSize);

        if (dataSend < 0) {
            std::cerr << "Error in sending data." << std::endl;
        }
       /* else {
            std::cout << "sent value: " << position.counter << "\n";
        }*/

}
```

Listing A.3: C++ code used on PC to receive information from the RT PC generate a force and apply it at the Falcon

```
//RECEIVE the force from FLEXENDOCAB and apply it to the falcon:

            int dataRead = recvfrom(udpSocket, reinterpret_cast<char*>(&torque),
            sizeof(torque), 0, (struct sockaddr*)
            &RemoteAddress,
            &RemoteAddressSize);
            int error = WSAGetLastError();

            if (dataRead < 0) {
                std::cerr << "Error in receving data." << std::endl;
            }
            /*else {
                std::cout << "Received value: " <<force.a << "\n";
             }*/

            double force;
            double gain;



               //forcefeedback happens only when pushing button

               if (userbutton == 1) {

                   if (abs(torque.a) < 0.001) {
                       force = 0;
                   }
                   else {

                       // forces(1-11) torques(1.5e-3, 5.5e-3)

                       //POWER2
                       gain = 333333.33 * abs(torque.a) + 166.67;
                       int sign = torque.a / abs(torque.a);
                       force = sign * gain * abs(torque.a);


                   }
               }
               else {

                   force = 0;
```

```
    }


    forcesarray.push_back(force);
    countarray.push_back(position.counter);



    //print force even if it's not applied directly
    //ABLED ONLY WHEN NO FEEDBACK
printf(" % +0.03f", force);

// set and print force
//ABLED ONLY WHEN FEEDBACK
    if (dhdSetForce(0, 0, force) < DHD_NO_ERROR) {
        printf("error:cannot set force (%s)\n", dhdErrorGetLastStr());
        done = 1;

    }
    else {
        printf(" % +0.03f", force);
    }
```

B Appendix

In the following appendix the plots for the other axis (x-axis and z-axis) are reposrted, that were not included in 4.

B.1 Step function

Centre of workspace

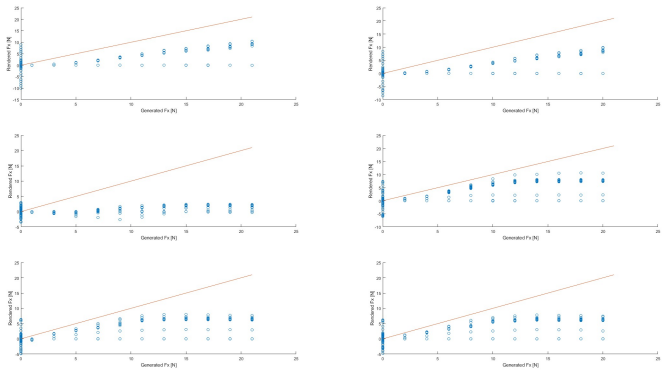

Figure B.1: Scatter-plot of the step function at the centre of the work space for all the sent functions. First row x-axis, second row y-axis, third row z-axis. Left plots odd steps, right plots even steps

Y- and z-axis limit of workspace

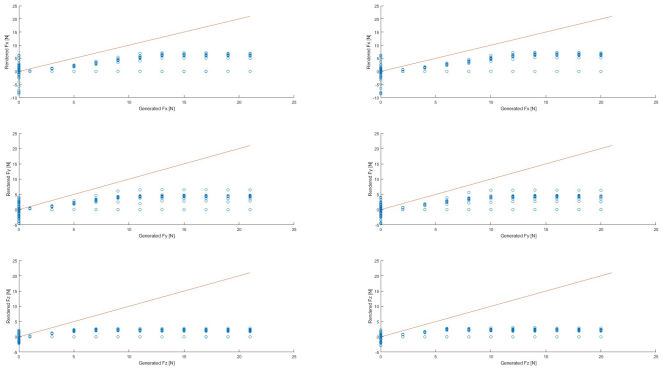

Figure B.2: Scatter-plot of the step function at the limit of the workspace for y- and z-axis for all the sent functions. First row x-axis, second row y-axis, third row z-axis. Left plots odd steps, right plots even steps

X-axis limit of workspace

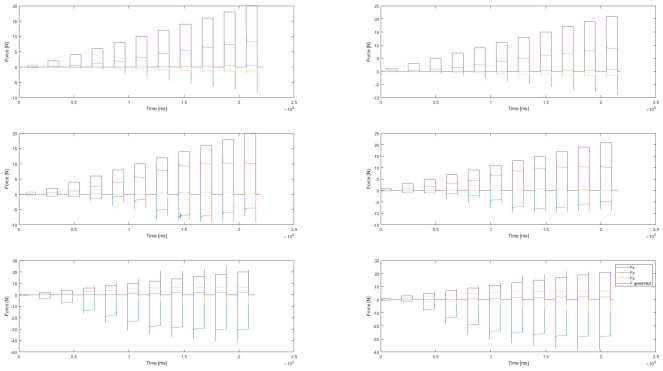

Figure B.3: Step function along all the tree axes. X-axis top, y-axis middle, z-axis bottom.

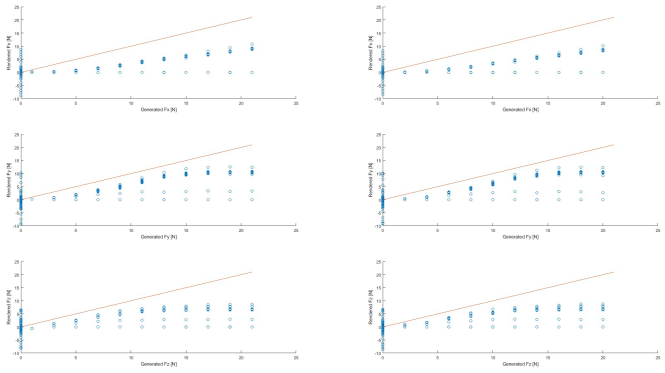

Figure B.4: Scatter-plot of the step function at the limit of the workspace for x-axis for all the sent functions. First row x-axis, second row y-axis, third row z-axis. Left plots odd steps, right plots even steps

B.2 Sine waves

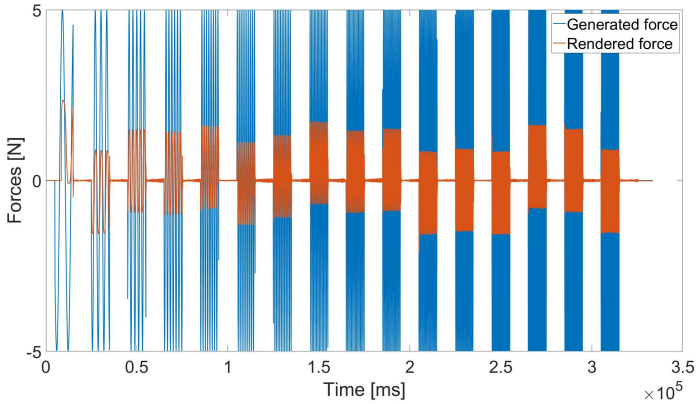

Figure B.5: Plot of generated and rendered forces when applying a sine wave with a fixed amplitude and an incremental frequency on the x-axis.

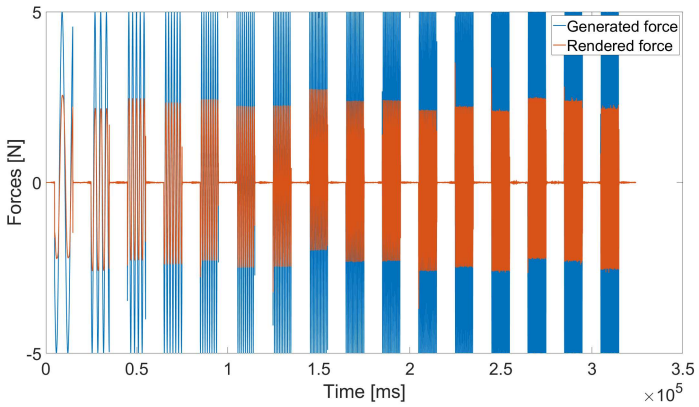

Figure B.6: Plot of generated and rendered forces when applying a sine wave with a fixed amplitude and an incremental frequency on the z-axis.

C Appendix

In the following appendix the answers of the users to the user study can be found.
for each participant in the column user# the decision for the single inspection was reported (0 being soft tissue, 1 being hard tissue). In the column resultuser# the difference between the column user# and the one with the actual stiffness was reported (0 being correct detection, 1 detected hard when soft, -1 detected soft when hard). In the last rows for each participant, the answer to the questions in Chap. 5.

legend: (1=insertion, 0=no insertion)
result =0 => correct answer
result =1 => detected hard when soft
result=-1 => detected soft when hard

test		user1	resultuser1		user2	resultuser2		user3	resultuser3
0		11	11		1	1		1	1
1		1	0		1	0		11	10
1		0	-1		0	-1		0	-1
0		1	1		1	1		0	0
1		0	-1		0	-1		0	-1
0		1	1		1	1		1	1
1		0	-1		0	-1		0	-1
0			0			0			0
NHF									
0		0	0		0	0		0	0
1		1	0		0	-1		1	0
1		1	0		1	0		1	0
0		0	0		0	0		0	0
1		1	0		1	0		1	0
1		1	0		1	0		1	0
1		1	0		1	0		1	0
0		0	0		1	1		0	0
HF									
1		1	0		1	0		1	0
0		0	0		1	1		0	0
1		1	0		1	0		1	0
1		1	0		1	0		1	0
0		0	0		0	0		0	0
1		1	0		1	0		1	0
1		1	0		1	0		1	0
0		0	0		0	0		0	0
First NHF or HF?			Hf			Nhf			Nhf
question1			78			4 7			6 8
question2			4			4			4
question3									
question4			Less			Less			More
question5			Low			Same			Less

Figure C.1: Excel table showing results of the user study.

user4	resultuser4		user5	resultuser5		user6	redultuser6		user7	resultuser7
1	1		1	1		1	1		1	1
1	0		1	0		1	0		11	10
0	-1		0	-1		0	-1		0	-1
0	0		1	1		1	1		1	1
0	-1		0	-1		0	-1		0	-1
1	1		1	1		1	1		1	1
0	-1		0	-1		0	-1		1	0
	0			0			0			0
0	0		0	0		0	0		0	0
1	0		1	0		1	0		1	0
1	0		1	0		1	0		1	0
0	0		0	0		0	0		0	0
1	0		1	0		1	0		0	-1
1	0		1	0		1	0		1	0
1	0		1	0		0	-1		0	-1
0	0		0	0		0	0		0	0
0	-1		1	0		1	0		1	0
0	0		0	0		0	0		0	0
1	0		1	0		0	-1		1	0
1	0		1	0		1	0		1	0
0	0		0	0		0	0		0	0
1	0		1	0		1	0		1	0
1	0		1	0		1	0		1	0
0	0		0	0		1	1		0	0
	Nhf			Hf			Hf			Nhf
	54			68			55			58
	3			4			4			4
	Less			Less			Less			Less
	Don't know			Less			Don't know			Less

Figure C.2: Excel table showing results of the user study.

user8	resultuser8		User9	Resultuser9		user10	resultuser10
1	1		1	1		1	1
11	10		11	10		11	10
0	-1		0	-1		0	-1
1	1		1	1		1	1
0	-1		0	-1		0	-1
1	1		1	1		1	1
0	-1		0	-1		1	0
	0			0			0
0	0		0	0		0	0
1	0		1	0		1	0
1	0		1	0		0	-1
0	0		0	0		0	0
1	0		1	0		1	0
1	0		1	0		1	0
1	0		1	0		1	0
0	0		0	0		0	0
1	0		1	0		1	0
0	0		0	0		0	0
1	0		1	0		1	0
1	0		1	0		1	0
0	0		0	0		0	0
1	0		1	0		1	0
1	0		1	0		1	0
0	0		0	0		0	0
	Hf			Nhf			Hf
	68			76			78
	4			4			5
	Less			Less			same
	Don't know			Less			less

Figure C.3: Excel table showing results of the user study.

Bibliography

[1] "Safer robotic endoscopy with inspiration from the human fnger," 2023.

[2] P. Puangmali, K. Althoefer, L. D. Seneviratne, D. Murphy, and P. Dasgupta, "State-of-the-art in force and tactile sensing for minimally invasive surgery," *IEEE Sensors Journal*, vol. 8, no. 4, pp. 371–381, 2008.

[3] A. S. Naidu, M. D. Naish, and R. V. Patel, "A breakthrough in tumor localization: Combining tactile sensing and ultrasound to improve tumor localization in robotics-assisted minimally invasive surgery," *IEEE Robotics & Automation Magazine*, vol. 24, no. 2, pp. 54–62, 2017.

[4] W. Kraus, M. Kessler, and A. Pott, "Pulley friction compensation for winch-integrated cable force measurement and verification on a cable-driven parallel robot," in *2015 IEEE International Conference on Robotics and Automation (ICRA)*, pp. 1627–1632, IEEE, 2015.

[5] L. Fasel, N. Gerig, A. Danun, M. Meboldt, R. Guzman, P. C. Cattin, and G. Rauter, "Antagonistic series elastic actuation for a variable stiffness robotic endoscope," *[unpublished]*, 2024.

[6] A. K. Golahmadi, D. Z. Khan, G. P. Mylonas, and H. J. Marcus, "Tool-tissue forces in surgery: A systematic review," *Annals of Medicine and Surgery*, vol. 65, p. 102268, 2021.

[7] M. C. Dewan, A. Rattani, G. Fieggen, M. A. Arraez, F. Servadei, F. A. Boop, W. D. Johnson, B. C. Warf, and K. B. Park, "Global neurosurgery: the current capacity and deficit in the provision of essential neurosurgical care. executive summary of the global neurosurgery initiative at the program in global surgery and social change," *Journal of neurosurgery*, vol. 130, no. 4, pp. 1055–1064, 2018.

[8] D. Korolija, S. Sauerland, S. Wood-Dauphinee, C. Abbou, E. Eypasch, M. G. Caballero, M. Lumsden, B. Millat, J. Monson, G. Nilsson, *et al.*, "Evaluation of quality of

life after laparoscopic surgery: evidence-based guidelines of the european association for endoscopic surgery," *Surgical endoscopy*, vol. 18, pp. 879–897, 2004.

[9] H. Muaddi, M. El Hafid, W. J. Choi, E. Lillie, C. de Mestral, A. Nathens, T. A. Stukel, and P. J. Karanicolas, "Clinical outcomes of robotic surgery compared to conventional surgical approaches (laparoscopic or open): a systematic overview of reviews," *Annals of surgery*, vol. 273, no. 3, pp. 467–473, 2021.

[10] K. Veluvolu and W. Ang, "Estimation and filtering of physiological tremor for real-time compensation in surgical robotics applications," *The International Journal of Medical Robotics and Computer Assisted Surgery*, vol. 6, no. 3, pp. 334–342, 2010.

[11] R. D. Howe and Y. Matsuoka, "Robotics for surgery," *Annual review of biomedical engineering*, vol. 1, no. 1, pp. 211–240, 1999.

[12] I. J. Y. Wee, L.-J. Kuo, and J. C.-Y. Ngu, "A systematic review of the true benefit of robotic surgery: Ergonomics," *The international journal of medical robotics and computer assisted surgery*, vol. 16, no. 4, p. e2113, 2020.

[13] S. Maeso, M. Reza, J. A. Mayol, J. A. Blasco, M. Guerra, E. Andradas, and M. N. Plana, "Efficacy of the da vinci surgical system in abdominal surgery compared with that of laparoscopy: a systematic review and meta-analysis," *Annals of surgery*, vol. 252, no. 2, pp. 254–262, 2010.

[14] C. Freschi, V. Ferrari, F. Melfi, M. Ferrari, F. Mosca, and A. Cuschieri, "Technical review of the da vinci surgical telemanipulator," *The International Journal of Medical Robotics and Computer Assisted Surgery*, vol. 9, no. 4, pp. 396–406, 2013.

[15] L. S. Mattos, D. G. Caldwell, G. Peretti, F. Mora, L. Guastini, and R. Cingolani, "Microsurgery robots: addressing the needs of high-precision surgical interventions," *Swiss medical weekly*, vol. 146, no. 4344, pp. w14375–w14375, 2016.

[16] A. M. Okamura, "Haptic feedback in robot-assisted minimally invasive surgery," *Current opinion in urology*, vol. 19, no. 1, p. 102, 2009.

[17] A. Pandya, S. Eslamian, H. Ying, M. Nokleby, and L. A. Reisner, "A robotic recording and playback platform for training surgeons and learning autonomous behaviors using the da vinci surgical system," *Robotics*, vol. 8, no. 1, p. 9, 2019.

[18] Y. S. Kwoh, J. Hou, E. A. Jonckheere, and S. Hayati, "A robot with improved absolute positioning accuracy for ct guided stereotactic brain surgery," *IEEE transactions on biomedical engineering*, vol. 35, no. 2, pp. 153–160, 1988.

[19] A. R. Lanfranco, A. E. Castellanos, J. P. Desai, and W. C. Meyers, "Robotic surgery: a current perspective," *Annals of surgery*, vol. 239, no. 1, pp. 14–21, 2004.

[20] M. Diana and J. Marescaux, "Robotic surgery," *Journal of British Surgery*, vol. 102, no. 2, pp. e15–e28, 2015.

[21] I. El Rassi and J.-M. El Rassi, "A review of haptic feedback in tele-operated robotic surgery," *Journal of medical engineering & technology*, vol. 44, no. 5, pp. 247–254, 2020.

[22] R. V. Patel, S. F. Atashzar, and M. Tavakoli, "Haptic feedback and force-based teleoperation in surgical robotics," *Proceedings of the IEEE*, vol. 110, no. 7, pp. 1012–1027, 2022.

[23] C. Pacchierotti, L. Meli, F. Chinello, M. Malvezzi, and D. Prattichizzo, "Cutaneous haptic feedback to ensure the stability of robotic teleoperation systems," *The International Journal of Robotics Research*, vol. 34, no. 14, pp. 1773–1787, 2015.

[24] C. Pacchierotti, A. Tirmizi, and D. Prattichizzo, "Improving transparency in teleoperation by means of cutaneous tactile force feedback," *ACM Transactions on Applied Perception (TAP)*, vol. 11, no. 1, pp. 1–16, 2014.

[25] D. Prattichizzo, C. Pacchierotti, and G. Rosati, "Cutaneous force feedback as a sensory subtraction technique in haptics," *IEEE Transactions on Haptics*, vol. 5, no. 4, pp. 289–300, 2012.

[26] E. P. Scilingo, M. Bianchi, G. Grioli, and A. Bicchi, "Rendering softness: Integration of kinesthetic and cutaneous information in a haptic device," *IEEE Transactions on Haptics*, vol. 3, no. 2, pp. 109–118, 2010.

[27] B. T. Bethea, A. M. Okamura, M. Kitagawa, T. P. Fitton, S. M. Cattaneo, V. L. Gott, W. A. Baumgartner, and D. D. Yuh, "Application of haptic feedback to robotic surgery," *Journal of Laparoendoscopic & Advanced Surgical Techniques*, vol. 14, no. 3, pp. 191–195, 2004.

[28] M. Bergholz, M. Ferle, and B. M. Weber, "The benefits of haptic feedback in robot assisted surgery and their moderators: a meta-analysis," *Scientific Reports*, vol. 13, no. 1, p. 19215, 2023.

[29] O. A. Van der Meijden and M. P. Schijven, "The value of haptic feedback in conventional and robot-assisted minimal invasive surgery and virtual reality training: a current review," *Surgical endoscopy*, vol. 23, pp. 1180–1190, 2009.

[30] A. Pressman, L. J. Welty, A. Karniel, and F. A. Mussa-Ivaldi, "Perception of delayed stiffness," *The International Journal of Robotics Research*, vol. 26, no. 11-12, pp. 1191–1203, 2007.

[31] I. Nisky, F. A. Mussa-Ivaldi, and A. Karniel, "A regression and boundary-crossing-based model for the perception of delayed stiffness," *IEEE Transactions on Haptics*, vol. 1, no. 2, pp. 73–82, 2008.

[32] S. Hirche and M. Buss, "Human perceived transparency with time delay," in *Advances in Telerobotics*, pp. 191–209, Springer, 2007.

[33] W. Fu, M. M. van Paassen, D. A. Abbink, and M. Mulder, "Framework for human haptic perception with delayed force feedback," *IEEE Transactions on Human-Machine Systems*, vol. 49, no. 2, pp. 171–182, 2018.

[34] J. Han, J. Davids, H. Ashrafian, A. Darzi, D. S. Elson, and M. Sodergren, "A systematic review of robotic surgery: From supervised paradigms to fully autonomous robotic approaches," *The International Journal of Medical Robotics and Computer Assisted Surgery*, vol. 18, no. 2, p. e2358, 2022.

[35] L. S. Gan, K. Zareinia, S. Lama, Y. Maddahi, F. W. Yang, and G. R. Sutherland, "Quantification of forces during a neurosurgical procedure: A pilot study," *World neurosurgery*, vol. 84, no. 2, pp. 537–548, 2015.

[36] N. Enayati, E. De Momi, and G. Ferrigno, "Haptics in robot-assisted surgery: Challenges and benefits," *IEEE reviews in biomedical engineering*, vol. 9, pp. 49–65, 2016.

[37] M. Mahvash, J. Gwilliam, R. Agarwal, B. Vagvolgyi, L.-M. Su, D. D. Yuh, and A. M. Okamura, "Force-feedback surgical teleoperator: Controller design and palpation experiments," in *2008 Symposium on Haptic Interfaces for Virtual Environment and Teleoperator Systems*, pp. 465–471, IEEE, 2008.

[38] P. Schleer, P. Kaiser, S. Drobinsky, and K. Radermacher, "Augmentation of haptic feedback for teleoperated robotic surgery," *International Journal of Computer Assisted Radiology and Surgery*, vol. 15, pp. 515–529, 2020.

[39] L. Seminara, P. Gastaldo, S. J. Watt, K. F. Valyear, F. Zuher, and F. Mastrogiovanni, "Active haptic perception in robots: a review," *Frontiers in neurorobotics*, vol. 13, p. 53, 2019.

[40] E. Abdi, D. Kulić, and E. Croft, "Haptics in teleoperated medical interventions: force measurement, haptic interfaces and their influence on user's performance," *IEEE Transactions on Biomedical Engineering*, vol. 67, no. 12, pp. 3438–3451, 2020.

[41] A. Srivastava, R. Xu, A. Escoto, C. Ward, and R. V. Patel, "Design of an ultra thin strain sensor using superelastic nitinol for applications in minimally invasive surgery," in *2016 IEEE International Conference on Advanced Intelligent Mechatronics (AIM)*, pp. 794–799, IEEE, 2016.

[42] A. S. Naidu, R. V. Patel, and M. D. Naish, "Low-cost disposable tactile sensors for palpation in minimally invasive surgery," *IEEE/ASME Transactions on Mechatronics*, vol. 22, no. 1, pp. 127–137, 2016.

[43] Z. Chua, A. M. Jarc, and A. M. Okamura, "Toward force estimation in robot-assisted surgery using deep learning with vision and robot state," in *2021 IEEE International Conference on Robotics and Automation (ICRA)*, pp. 12335–12341, IEEE, 2021.

[44] M. Haghighipanah, M. Miyasaka, and B. Hannaford, "Utilizing elasticity of cable-driven surgical robot to estimate cable tension and external force," *IEEE Robotics and Automation Letters*, vol. 2, no. 3, pp. 1593–1600, 2017.

[45] H. Sang, J. Yun, R. Monfaredi, E. Wilson, H. Fooladi, and K. Cleary, "External force estimation and implementation in robotically assisted minimally invasive surgery," *The International Journal of Medical Robotics and Computer Assisted Surgery*, vol. 13, no. 2, p. e1824, 2017.

[46] W. Lai, L. Cao, R. X. Tan, Y. C. Tan, X. Li, P. T. Phan, A. M. H. Tiong, S. C. Tjin, and S. J. Phee, "An integrated sensor-model approach for haptic feedback of flexible endoscopic robots," *Annals of Biomedical Engineering*, vol. 48, pp. 342–356, 2020.

[47] L. Fasel, N. Gerig, P. C. Cattin, and G. Rauter, "The sea-scope: Torque-limited endoscopic joint control for telemanipulation or visual servoing through tendon force control with series elastic actuation," in *2021 International Symposium on Medical Robotics (ISMR)*, pp. 1–7, IEEE, 2021.

[48] L. Fasel, N. Gerig, P. C. Cattin, and G. Rauter, "Control evaluation of antagonistic series elastic actuation for a robotic endoscope joint," *Journal of Bionic Engineering*, vol. 19, no. 4, pp. 965–974, 2022.

[49] C. R. Wottawa, B. Genovese, B. N. Nowroozi, S. D. Hart, J. W. Bisley, W. S. Grundfest, and E. P. Dutson, "Evaluating tactile feedback in robotic surgery for potential clinical application using an animal model," *Surgical endoscopy*, vol. 30, pp. 3198–3209, 2016.

[50] K. Feng, Q. Xu, and L. M. Tam, "Design and development of a dexterous bilateral robotic microinjection system based on haptic feedback," *IEEE Transactions on Automation Science and Engineering*, vol. 20, no. 2, pp. 1452–1462, 2022.

[51] A. Pott and T. Bruckmann, *Cable-driven parallel robots*. Springer, 2013.

[52] V. Hayward, O. R. Astley, M. Cruz-Hernandez, D. Grant, and G. Robles-De-La-Torre, "Haptic interfaces and devices," *Sensor review*, vol. 24, no. 1, pp. 16–29, 2004.

[53] S. Martin and N. Hillier, "Characterisation of the novint falcon haptic device for application as a robot manipulator," in *Australasian Conference on Robotics and Automation (ACRA)*, pp. 291–292, Citeseer, 2009.

[54] C. Salisbury, R. B. Gillespie, H. Z. Tan, F. Barbagli, and J. K. Salisbury, "What you can't feel won't hurt you: Evaluating haptic hardware using a haptic contrast sensitivity function," *IEEE Transactions on Haptics*, vol. 4, no. 2, pp. 134–146, 2011.

[55] T. Wang, B. Pan, Y. Fu, S. Wang, and Y. Ai, "Design of a new haptic device and experiments in minimally invasive surgical robot," *Computer Assisted Surgery*, vol. 22, no. sup1, pp. 240–250, 2017.

[56] N. Najmaei, A. Asadian, M. R. Kermani, and R. V. Patel, "Design and performance evaluation of a prototype mrf-based haptic interface for medical applications," *IEEE/ASME Transactions on Mechatronics*, vol. 21, no. 1, pp. 110–121, 2015.

[57] R. Wirz, M. Ferre, R. Marín, J. Barrio, J. M. Claver, and J. Ortego, "Efficient transport protocol for networked haptics applications," in *Haptics: Perception, Devices and Scenarios: 6th International Conference, EuroHaptics 2008 Madrid, Spain, June 10-13, 2008 Proceedings 6*, pp. 3–12, Springer, 2008.

[58] R. M. Traylor, D. Wilhelm, B. D. Adelstein, and H. Z. Tan, "Design considerations for stand-alone haptic interfaces communicating via udp protocol," in *First Joint Eurohaptics Conference and Symposium on Haptic Interfaces for Virtual Environment and Teleoperator Systems. World Haptics Conference*, pp. 563–564, IEEE, 2005.

[59] L. Fasel, N. Gerig, P. C. Cattin, and G. Rauter, "Tendon force control evaluation for an endoscope with series elastic actuation," in *New Trends in Medical and Service Robotics: MESROB 2020 7*, pp. 118–126, Springer, 2021.

[60] G. A. Pratt and M. M. Williamson, "Series elastic actuators," in *Proceedings 1995 IEEE/RSJ International Conference on Intelligent Robots and Systems. Human Robot Interaction and Cooperative Robots*, vol. 1, pp. 399–406, IEEE, 1995.

[61] A. Albakri, *Haptic Teleoperation for Robotic-Assisted Surgery*. PhD thesis, 2015.

[62] S. Budday, T. C. Ovaert, G. A. Holzapfel, P. Steinmann, and E. Kuhl, "Fifty shades of brain: a review on the mechanical testing and modeling of brain tissue," *Archives of Computational Methods in Engineering*, vol. 27, pp. 1187–1230, 2020.

[63] S. Budday, G. Sommer, C. Birkl, C. Langkammer, J. Haybaeck, J. Kohnert, M. Bauer, F. Paulsen, P. Steinmann, E. Kuhl, *et al.*, "Mechanical characterization of human brain tissue," *Acta biomaterialia*, vol. 48, pp. 319–340, 2017.

[64] A. Tejo-Otero, F. Fenollosa-Artés, I. Achaerandio, S. Rey-Vinolas, I. Buj-Corral, M. Á. Mateos-Timoneda, and E. Engel, "Soft-tissue-mimicking using hydrogels for the development of phantoms," *Gels*, vol. 8, no. 1, p. 40, 2022.

[65] M. C. Yip, M. Tavakoli, and R. D. Howe, "Performance analysis of a haptic telemanipulation task under time delay," *Advanced Robotics*, vol. 25, no. 5, pp. 651–673, 2011.

[66] R. Nomberg and I. Nisky, "Human stabilization of delay-induced instability of haptic rendering in a stiffness discrimination task," *IEEE Transactions on Haptics*, vol. 16, no. 1, pp. 33–45, 2022.

[67] C. A. S. (2024), "Normal distribution analyser, matlab central file exchange." https://www.mathworks.com/matlabcentral/fileexchange/134032-normal-distribution-analyser), 2021. [Online; Retrieved March 18, 2024].

[68] S. S. Shapiro and M. B. Wilk, "An analysis of variance test for normality (complete samples)," *Biometrika*, vol. 52, no. 3-4, pp. 591–611, 1965.